



# Project Reports 2025 - 2026

**Lead Institution:**

The University of Tennessee Knoxville

**Core Partner Institutions:**

Northeastern University

Rensselaer Polytechnic Institute

Tuskegee University

# Table of Contents

Power Systems.....	4
1. DG Siting and Sizing Considering Energy Vulnerability .....	5
2. Mitigation of Circular Flows in HVDC-Integrated Transmission Systems\.....	7
3. Resilience-Oriented Scenario Reduction and Assessment under Extreme Events .....	10
4. ADMM-based Virtual Inertia Scheduling (VIS) to Preserve Privacy in Networked Microgrids.....	12
5. PVSizer: An Open-Source Python Framework for PV and BESS Sizing in Distribution Networks.....	14
6. Measurement-informed Dynamic Aggregation of Distribution Systems .....	16
7. Acoustic UAV Detection at Electrical Power Substations Using a Harmonic Signature Tracking Method.....	17
8. Development of Load Flexibility Valuation Methodology & Framework to Input into System Planning Tools .....	19
9. Enhanced Online Oscillation Detection Framework for Sub-Synchronous Oscillation (SSO) 21	
10. Wide-Area Oscillation Damping Control Using FACTS as Actuators: TERNA Case Study 23	
11. Frequency Response of Windowed DFT Phasor Estimation: Impact on Oscillation Observability.....	25
12. OEDI – Solar Grid Integration Data and Analytics Library .....	28
13. Real-Time Local Damping of Wideband Power Oscillations Using Droop-Controlled IBRs 29	
14. Large-Scale Data Center Load Modeling With Real Event Scenario .....	31
15. Detection of Large Load Loss Event: Focus on the Northern Virginia Data Center Hub 33	
16. Bridging PMU Measurements and Dynamic Simulation for Oscillation Analysis .....	34
17. A Heterogeneous Multiscale Method for Efficient Simulation of Power Systems with Inverter-Based Resources .....	36
18. PowerCascade: Power Systems Cascading Failure Analysis Synthetic Dataset.....	38
19. Variable Time-Step Optimal Order Differential Transformation for Power System with IBR 40	
20. A Voronoi Diagram-Based Approach for AC Optimal Power Flow .....	42

<b>Power Electronics</b> .....	44
21. Assessing Grid Reliability Limits for Urban Air Mobility Integration.....	45
22. Integrated Three-level GaN Inverter and PMSynRM Motor for Electric Passenger Vehicles and Medium/heavy duty Trucks (GaNIn_PMSynRM) .....	47
23. Characterization of DFPACK and Evaluation of DFPACK in an Inverter Application.....	48
24. Characterization of HV bi-directional GaN devices and development of 22kW bidirectional GaN devices based three-phase single-stage wireless battery charger for electric vehicles .....	49
25. A High-efficiency and High-power-density 48/12V DC/DC Converter for Electric Vehicles.....	50
26. A GaN based DC/DC Converter Using Planar Technology for Electric Vehicles .....	51
27. Integrated Zero-Emission Aviation using a Robust Hybrid Architecture.....	52
28. Multi-Input Integrated Smart Charger-Inverter System for Electric Vehicles.....	53
29. Electric Machines with Adaptive Surge Impedance .....	54
30. Advanced Immersion Cooled Power Electronic Converters.....	55
31. Digital Twin Predictive Health Monitoring of Solid-State Transformers.....	56
32. Multiport Quad-Active-Bridge Converters for PV-Battery-EV-Grid Systems.....	57
33. A Generalized Physics-Based Circuit Model for Predicting Nonlinear Properties of Magnetic Materials. ....	58
34. Co-located SMRs, hyperscale data centers, and energy storage for increased system resiliency .....	60
35. An Ultra-Light Tightly-Integrated Modular Aviation Transportation Enabling Solid-State Circuit Breaker (ULTIMATE-SSCB).....	62
36. A UNIVERSAL (Ultrafast, Noise-Immune, Versatile, Efficient, Reliable, Scalable, and Accurate Light-controlled) Switch Module .....	64
37. SiC Based Modular Transformer-Less MW-Scale Power Conditioning System and Controller for Flexible Manufacturing Plants .....	66
38. High Performance Isolated Dc/Dc Converter For Future Hvdc Data Center Application	

# **Power Systems**

## 1. DG Siting and Sizing Considering Energy Vulnerability

<b>Project Lead:</b> Fran Li (UTK)
<b>Graduate Students and Research faculty/associates:</b> Chenchen Li (UTK)
<b>Project Duration:</b> 10/2024 – 12/2025
<b>Funding Source:</b> DOE – EARNEST, Stanford University

### Summary

This project aims to develop a generalized approach for distributed generator (DG) siting and sizing to improve system resilience and reduce energy vulnerability. However, a key challenge lies in the lack of a general metric to quantify energy vulnerability in power systems. Additionally, incorporating energy vulnerability into DG planning models remains a challenge.

This year, the proposed resilience-oriented DG siting and sizing approach with energy vulnerability constraints (EVCs), developed in our previous study, is applied to a larger system (i.e., IEEE 123-bus system) to demonstrate its scalability. The expected load shedding index (ELSI), defined as the ratio of the load shedding to the original load, is calculated for each community. Moreover, a violation variable is introduced to ensure model feasibility. Based on this formulation, a sensitivity analysis is conducted on the weights in the cost coefficient of the violation variable associated with low-income communities.

The results show that, when energy vulnerability is considered, DG units tend to be installed at buses with low-income communities or with a heavy average load. This leads to a relatively large percentage reduction in ELSI for these communities, demonstrating that the proposed approach can simultaneously improve system resilience and reduce energy vulnerability. In addition, DG installation strategies and corresponding ELSI under different EVCs are presented in TABLE I and Figure 1, while the results under different weights in cost coefficients of violation variable corresponding to low-income communities are shown in TABLE II and Figure 2. According to these results, the following generalized guidelines can be concluded.

- (1) An effective method to satisfy a stricter EVC is to install DG units in proximity of where the low-income communities are located.
- (2) Under a tighter EVC, the difference in the ELSI among different income communities is smaller, and the ELSI of all communities remains at a relatively low level. Additionally, there is a higher energy vulnerability cost with respect to the reference case of no EVC considered, and a greater share (%) of this cost in the expected cost of unserved load.
- (3) Placing excessive emphasis on minimizing the ELSI for low-income communities can lead to higher ELSI values for other non-low-income communities. This overreaction does not contribute to reducing the energy vulnerability of the power system.

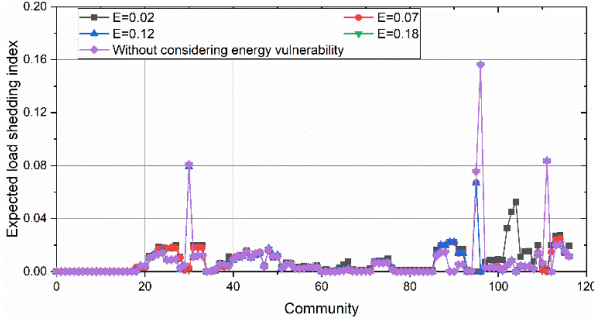


Figure 1: ELSI of the IEEE 123-bus system under different EVCs

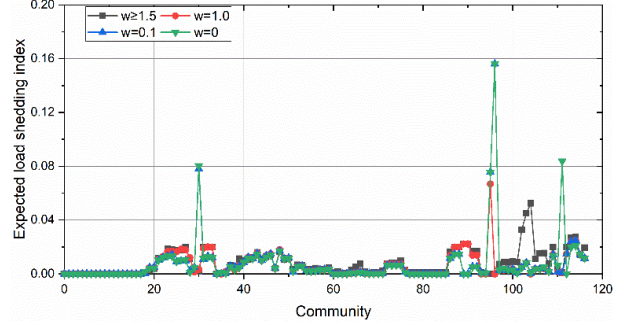


Figure 2: ELSI of the IEEE 123-bus system under different weights in cost coefficients of violation variable corresponding to low-income communities

TABLE I: Results of the IEEE 123-bus System Under Different EVCs.

Cases	DG unit bus (#)	Rated power of DG units (MW)	Energy equity cost (\$)	Energy equity cost / Expected costs of unserved load
$E=0.02$	30, 51, 77, 95, 96, 111	3.0, 3.0, 3.0, 3.0, 1.9, 3.0	2985	37.17%
$E=0.07$	30, 51, 77, 96, 104, 111	3.0, 3.0, 2.8, 3.0, 2.7, 2.4	1100	17.90%
$E=0.12$	28, 51, 77, 96, 104, 112	3.0, 3.0, 2.8, 3.0, 2.1, 3.0	625	11.02%
$E=0.18$	28, 51, 77, 89, 104, 112	3.0, 3.0, 3.0, 3.0, 1.9, 3.0	0	0
EVC is not considered (i.e., $E = \infty$ )	28, 51, 77, 89, 104, 112	3.0, 3.0, 3.0, 3.0, 1.9, 3.0	0 (ref. case)	0 (ref. case)

Note: Bus numbers in green indicate low-income community buses.

TABLE II: Results of the IEEE 123-bus System Under Different Weights in Cost Coefficients of the Violation Variable Corresponding to Low-income Communities.

Cases	DG unit bus (#)	Rated power of DG units (MW)	Energy vulnerability cost (\$)	Energy vulnerability cost / Expected costs of unserved load
$w \geq 1.5$	30, 51, 77, 95, 96, 111	3.0, 3.0, 3.0, 3.0, 1.9, 3.0	2985	37.17%
$w = 1.0$	30, 51, 77, 96, 104, 111	3.0, 3.0, 2.8, 3.0, 2.7, 2.4	1100	17.90%
$w = 0.1$	28, 51, 77, 89, 104, 111	3.0, 3.0, 2.8, 3.0, 2.7, 2.4	15	0.30%
$w = 0$	28, 51, 77, 89, 104, 112	3.0, 3.0, 3.0, 3.0, 1.9, 3.0	0 (ref. case)	0 (ref. case)

Note: Bus numbers in green indicate low-income community buses.

## 2. Mitigation of Circular Flows in HVDC-Integrated Transmission Systems\

<b>Project Lead:</b> Fran Li (UTK)
<b>Graduate Students and Research faculty/associates:</b> Chenchen Li (UTK)
<b>Project Duration:</b> 10/2024 – 4/2026
<b>Funding Source:</b> National Laboratory of the Rockies (NLR)

### Summary

This project aims to develop a market clearing approach that incorporates for marginal loss price and mitigates the circular flows in HVDC-integrated transmission systems. Circular flows refer to abnormal loop flows between HVDC and AC lines, driven by negative generation offers, inaccurate power losses modeling, and binding transmission constraints. These flows may lead to operational and stability concerns in transmission systems. In addition, the proposed strategy must be seamlessly integrated into existing ISO/RTO market clearing frameworks, which are integrated with established operational procedures, regulatory requirements, and software infrastructure. In this context, an optimization-based strategy is developed to enhance the current market framework and effectively mitigate circular flow issues.

The framework of the optimization-based strategy for mitigating circular flows is illustrated in Fig. 1. It consists of two main steps: HVDC power flow determination and market clearing.

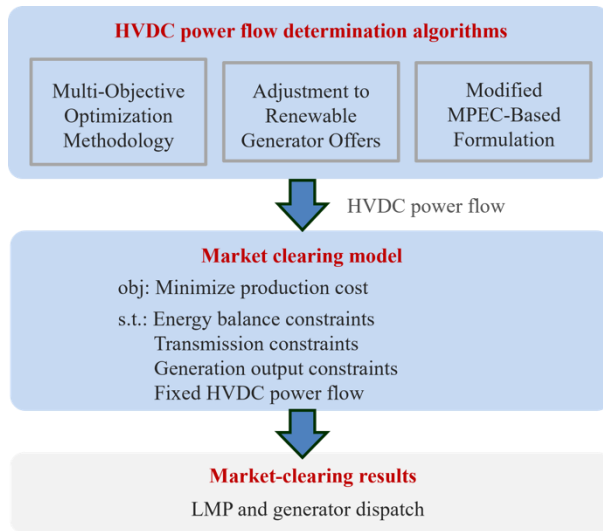


**Figure 1: The framework of optimization-based strategy for mitigating circular flows**

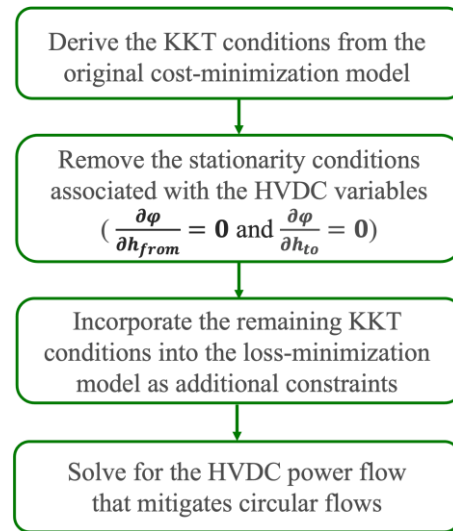


**Figure 2: The framework of modified MPEC-based formulations**

Several algorithms are proposed to determine HVDC power flows, including a multi-objective optimization methodology, an adjustment to renewable generator offers, and a modified mathematical program with equilibrium constraints (MPEC) based formulation. The multi-objective optimization methodology replaces the objective function in the original market clearing model with a weighted sum of production costs and system losses. The adjustment to renewable

generator offers removes subsidies for renewable generators, resulting in positive generation cost coefficients and preventing the artificial maximization of system losses. The modified MPEC-based formulation, as shown in Fig. 2, incorporates selected KKT conditions derived from the original cost-minimization model (excluding the stationarity conditions associated with HVDC variables) into a loss-minimization model as additional constraints. Solving these models yields HVDC power flows that avoid inducing circular flows. In the second step, the determined HVDC power flows are fixed in the ISO/RTO market clearing model, which is then solved to obtain the final locational marginal prices and generator dispatch.

The effectiveness of the proposed strategy is validated on a modified reliability test system developed by the National Laboratory of the Rockies (NLR), with case studies implemented in NLR's Sienna platform. The results of different algorithms under scenarios without and with binding transmission constraints are summarized in Table 1, from which the following conclusions can be drawn:

- (1) The multi-objective optimization methodology and the modified MPEC-based formulation effectively mitigate circular flows under both binding and non-binding transmission constraints. By explicitly considering system losses, the resulting HVDC power flow is below the critical threshold that does not induce circular flows.
- (2) The multi-objective optimization methodology achieves a relatively higher HVDC utilization rate, while the modified MPEC-based formulation leads to lower systems losses.
- (3) The adjustment to renewable generator offers mitigates circular flows only in the scenario without binding transmission constraints.

Overall, the proposed strategy provides system operators with a practical and flexible approach to mitigate circular flows in market clearing for HVDC-integrated transmission systems.

**Table 1: Results of different algorithms in different scenarios**

Algorithms	Without binding transmission constraints				With a binding transmission constraint			
	HVDC power flow (MW)	Production cost (\$)	System loss (MW)	Circular flow (yes or no)?	HVDC power flow (MW)	Production cost (\$)	System loss (MW)	Circular flow (yes or no)?
Cost-minimization	1218.96	93485.57	158.43	yes	1311.29	93489.25	175.11	yes
Loss-minimization	102.59	93503.22	44.02	no	102.59	93509.59	38.32	no
Enumeration method	480.00	93501.92	51.67	no	500.00	93507.26	48.27	no
Multi-objective optimization methodology	227.61	93503.55	42.05	no	267.56	93509.27	37.36	no
Adjustment to renewable generator offers	193.78	93503.54	42.11	no	593.07	93506.01	56.19	yes
Modified MPEC-based formulation	216.17	93503.56	42.03	no	204.30	93509.51	36.81	no

### 3. Resilience-Oriented Scenario Reduction and Assessment under Extreme Events

<b>Project Lead:</b> Fran Li (UTK)
<b>Graduate Students and Research faculty/associates:</b> Junjie Yin (UTK), Chenchen Li (UTK)
<b>Project Duration:</b> 10/2024 to 12/2025
<b>Funding Source:</b> DOE – EARNEST, Stanford University

#### Summary

The objective of this research is to develop a resilience-oriented scenario generation, reduction, and assessment framework for power systems under climate-driven extreme events. With the increasing frequency and severity of events such as torrential rainfall, hurricanes, and wildfires, conventional contingency analysis based on limited N–1 or predefined N–k conditions is no longer sufficient. Extreme events often induce spatially correlated outages and cascading failures, resulting in complex system responses that cannot be captured by traditional deterministic approaches. This study aims to establish a scalable framework that integrates probabilistic scenario generation, impact-based reduction, and multi-timescale assessment to enable efficient and accurate resilience evaluation.

As illustrated in Fig. 1, extreme events such as torrential rainfall can produce multiple potential hazard tracks, each associated with a distinct spatial footprint of system disruptions. These tracks define impacted zones, within which transmission and distribution assets may experience simultaneous outages. Unlike independent contingency assumptions, such geographically correlated failures significantly increase system vulnerability and can trigger large-scale disruptions. The proposed framework models these events by combining hazard trajectory representation with probabilistic failure mechanisms, enabling the generation of realistic large-scale N–k outage scenarios that capture both spatial dependency and uncertainty.

To address the computational challenges of massive scenario sets, a Monte Carlo-based scenario generation approach is adopted, followed by a two-stage assessment process. First, a static assessment layer performs rapid screening using steady-state power flow to evaluate key metrics such as load shedding, line loading, and voltage violations, thereby identifying high-impact scenarios and significantly reducing the candidate set. However, static metrics alone are insufficient to capture system resilience, especially in systems with high penetration of inverter-based resources. Therefore, selected scenarios undergo dynamic assessment through time-domain simulations to quantify transient stability metrics, including frequency deviation, RoCoF, and frequency nadir. This integrated evaluation ensures that scenarios with critical dynamic instability risks are retained, even if their steady-state impacts are moderate.

As shown in Fig. 2, a hybrid Monte Carlo–VAE–K-Medoids framework is proposed to extract representative scenarios from the reduced set. For each scenario, a feature vector is constructed by combining static and dynamic performance indicators, capturing both operational stress and stability characteristics. A Variational Autoencoder (VAE) is then employed to learn a compact latent representation of the high-dimensional feature space, preserving the intrinsic structure and similarity among scenarios. Subsequently, K-Medoids clustering is applied in the latent space to identify representative scenarios (medoids), ensuring that selected cases are physically meaningful

and robust to outliers. This approach enables a significant reduction in scenario size while maintaining the diversity and fidelity of system responses.

This research highlights the importance of jointly considering extreme-event characteristics, system vulnerability, and resilience metrics within a unified framework. By integrating probabilistic modeling, physics-based simulation, and data-driven learning, the proposed methodology provides an efficient pathway for identifying critical contingencies and evaluating system performance under extreme conditions.

In addressing future challenges, this study identifies several key research directions, including the incorporation of climate-informed failure models, improved representation of inverter-based resources, and the integration of physics-informed and data-driven approaches. Overall, this work contributes to the development of a scalable and adaptive resilience assessment framework for future power systems.

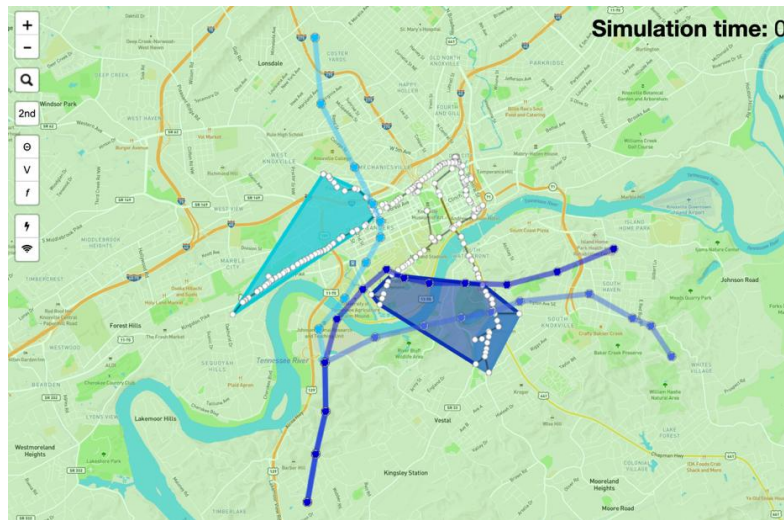


**Fig. 1. Illustration of torrential rainfall potential tracks and the corresponding impacted zones.**

---

**Algorithm 1** Monte Carlo–VAE–K-Medoids for Representative Scenario Extraction

---

- 1: Initialize line failure probabilities  $\{p_{ij}\}$  and convergence tolerance  $\varepsilon$
  - 2: Set sample size  $S \leftarrow 1000$ , previous estimate  $\hat{L}^{\text{prev}} \leftarrow \emptyset$ , and dataset  $\mathcal{D} \leftarrow \emptyset$
  - 3: **while** not converged **do**
  - 4:   Generate  $S$  outage scenarios via Monte Carlo simulation
  - 5:   **for** each scenario  $s = 1, \dots, S$  **do**
  - 6:     Determine outage topology and extract topology-based features
  - 7:     Run power flow under the sampled outage condition
  - 8:     Compute scenario features  $x_s$ , including load shed, maximum line loading, minimum voltage, imbalance, available inertia, RES penetration, and location encoding
  - 9:   **end for**
  - 10:   Update dataset  $\mathcal{D} \leftarrow \mathcal{D} \cup \{x_s\}_{s=1}^S$
  - 11:   Estimate expected load shed  $\hat{L} \leftarrow \frac{1}{S} \sum_{s=1}^S L_s$
  - 12:   **if**  $\hat{L}^{\text{prev}} \neq \emptyset$  and  $\frac{|\hat{L} - \hat{L}^{\text{prev}}|}{\hat{L}} < \varepsilon$  **then**
  - 13:     Stop Monte Carlo simulation
  - 14:   **else**
  - 15:     Set  $\hat{L}^{\text{prev}} \leftarrow \hat{L}$  and update  $S \leftarrow 2S$
  - 16:   **end if**
  - 17: **end while**
  - 18: Normalize feature vectors in dataset  $\mathcal{D}$
  - 19: Train a variational autoencoder (VAE) using  $\mathcal{D}$
  - 20: Encoder maps scenario feature  $x$  to latent parameters  $(\mu, \sigma)$  and samples latent vector  $z = \mu + \sigma\xi$ , where  $\xi \sim \mathcal{N}(0, I)$
  - 21: Decoder reconstructs  $\hat{x}$ , and VAE parameters are optimized using reconstruction loss and KL divergence
  - 22: Obtain latent representations  $\mathcal{Z} = \{z_i\}$  for all scenarios
  - 23: Apply K-Medoids clustering in latent space by minimizing  $\sum_i d(z_i, z_{m(k)})$
  - 24: Select medoid scenarios as representative scenarios
  - 25: **return** Representative scenarios and corresponding feature vectors
- 

**Fig. 2. Monte Carlo–VAE–K-Medoids Algorithm for Representative Scenario Extraction**

#### 4. ADMM-based Virtual Inertia Scheduling (VIS) to Preserve Privacy in Networked Microgrids

<b>Project Lead:</b> Fran Li (UTK)
<b>Graduate Students and Research faculty/associates:</b> Vince Wilson (UTK)
<b>Project Duration:</b> 2/2024 – 10/2025
<b>Funding Source:</b> ORNL

##### Summary

The objective of this project was two-fold. The first is to further develop an existing virtual inertia scheduling (VIS) economic dispatch mixed-integer linear program to enable multiple microgrid (MG) coordination and study inertia sharing between microgrids. The second objective is to use the multi-microgrid VIS to examine how different data sharing regimes between microgrids effects both internal control and the stability of multiple MG. The multi-MG VIS is solved using Gurobi while time domain simulations for dynamic verification and study are carried out using CURENT's ANDES platform.

The project consisted of three main tasks. The first was to expand the existing VIS formulation for microgrids to account for interchange of power between MG; this was done by applying the alternating direction method of multipliers to the standard VIS problem, splitting it into sub-problems each MG can solve independently. Next, variations in data privacy between microgrids will be examined by changing the type of data shared for constraint generation; frequency security constraints are affected by expected disturbance levels which are calculated based on contributions from each MG. By limiting the degree to which each MG shares information, the effect of different privacy regimes on scheduling results and dynamics can be examined. Real time dynamic simulations can be carried out using the ANDES platform to determine the validity of VIS solutions and examine changes in dynamic performance.

Work on this project from the optimization side is complete while dynamics validation requires more work. An ADMM formulation for VIS which uses novel nadir constraint linearization has been developed and can solve for shared dispatch, tie-line flows, virtual inertia and damping, and contingency reserves in a 5-microgrid version of the 123-bus test system. A sensitivity study comparing scheduling results between different ADMM formulations with varying privacy shows that levels of data sharing can meaningfully affect results. For dynamic validation of frequency constraints, the RoCoF constraint is held, showing successful distributed scheduling of inertia. Unfortunately, we are having difficulty getting the nadir constraint to hold and are investigating issues with our test case and/or ANDES workflow to find the issue.

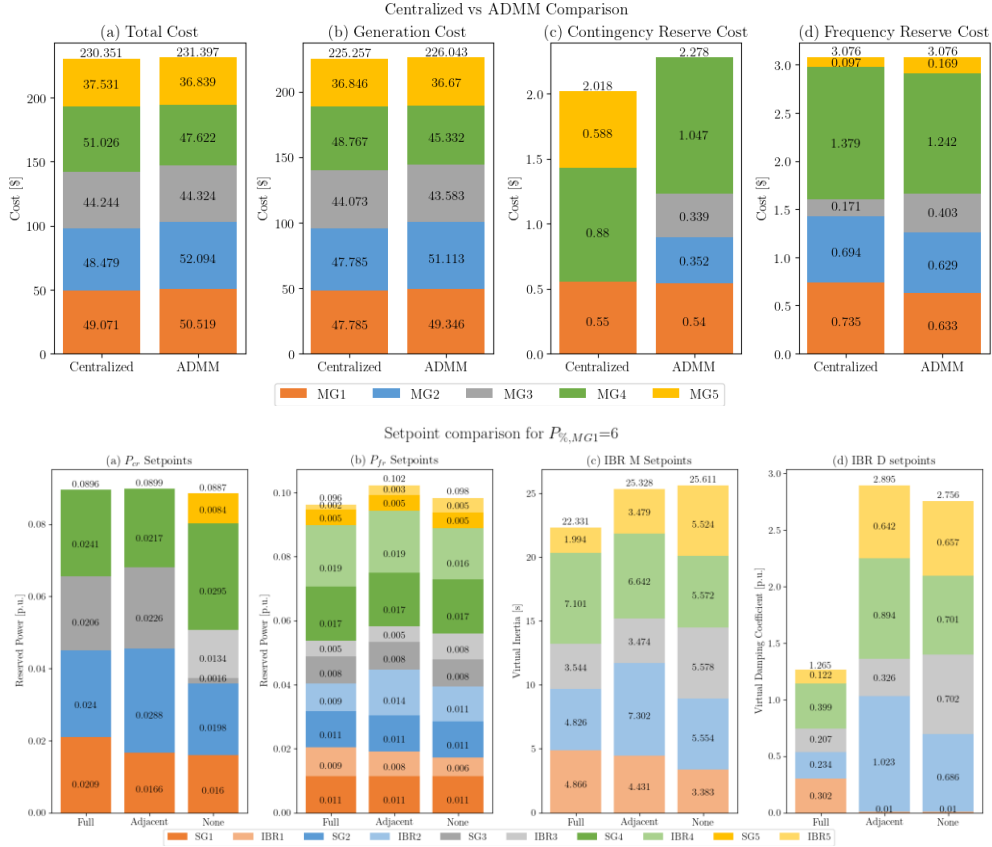


Figure 2: Scheduling results comparison for centralized vs ADMM solution and privacy sensitivity study

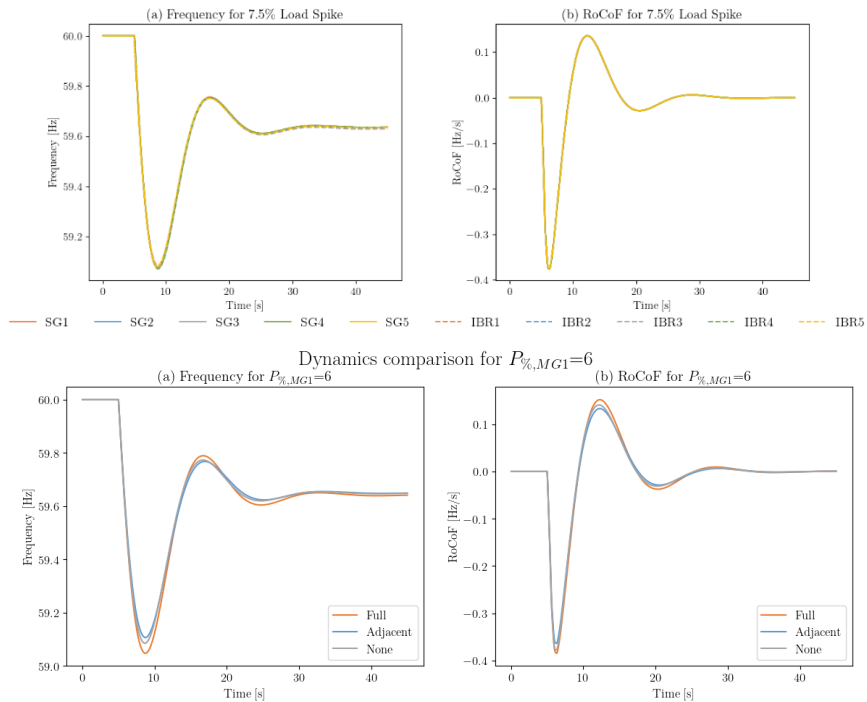


Figure 3: Dynamic results of base level ADMM-VIS dispatch and for privacy sensitivity study

## 5. PVSizer: An Open-Source Python Framework for PV and BESS Sizing in Distribution Networks

<b>Project Lead:</b> Yilu Liu (UTK) and Fran Li (UTK)
<b>Research Specialist:</b> Yayu(Andy) Yang (UTK)
<b>Project Duration:</b> 10/2024 – 10/2025
<b>Funding Source:</b> Department of Energy (DOE)

### Summary

**PVSizer** is a newly developed open-source Python framework designed to optimize the sizing of Photovoltaic (PV) systems and Battery Energy Storage Systems (BESS) within distribution networks. While originally motivated by the deployment of renewables on underutilized land such as retired landfills, the tool is versatile enough for preliminary sizing at any site. The primary objective is to maximize PV capacity while minimizing BESS requirements, ensuring that all local grid limits and stability constraints are maintained.

The framework is structured into three distinct analysis modules to cater to different planning needs:

- **Traversal/Feasibility map:** Tests all PV–BESS capacity combinations to map feasible operating regions.(Parallel Computing Architecture)
- **Quick solution:** Utilizes a hill-climbing algorithm to find the optimal PV and BESS sizes that meet all grid constraints.
- **Single test run:** Evaluate the impact of a specified-size PV and a specified-size BESS on the microgrid using 24-hour time series simulation.

The optimization logic focuses on maximizing the **PV rated active power** while determining the **minimum required BESS rated active power**.

To ensure grid reliability, the framework monitors several critical constraints: Power Flow Convergence; Voltage Limits; Thermal/ Loading Limits; Battery Capacity Constraints.

The effectiveness of PVSizer was demonstrated using a **Knoxville Utilities Board (KUB)** distribution feeder model. The tool successfully identified the feasibility frontier, mapping out where loading violations occur and where battery oversizing becomes unnecessary.

PVSizer is a newly developed PV and BESS design tool that maximizes PV size while minimizing BESS requirements within distribution system limits. It provides a tool for utilities, planners, and researchers to perform rigorous PV–BESS integration studies.

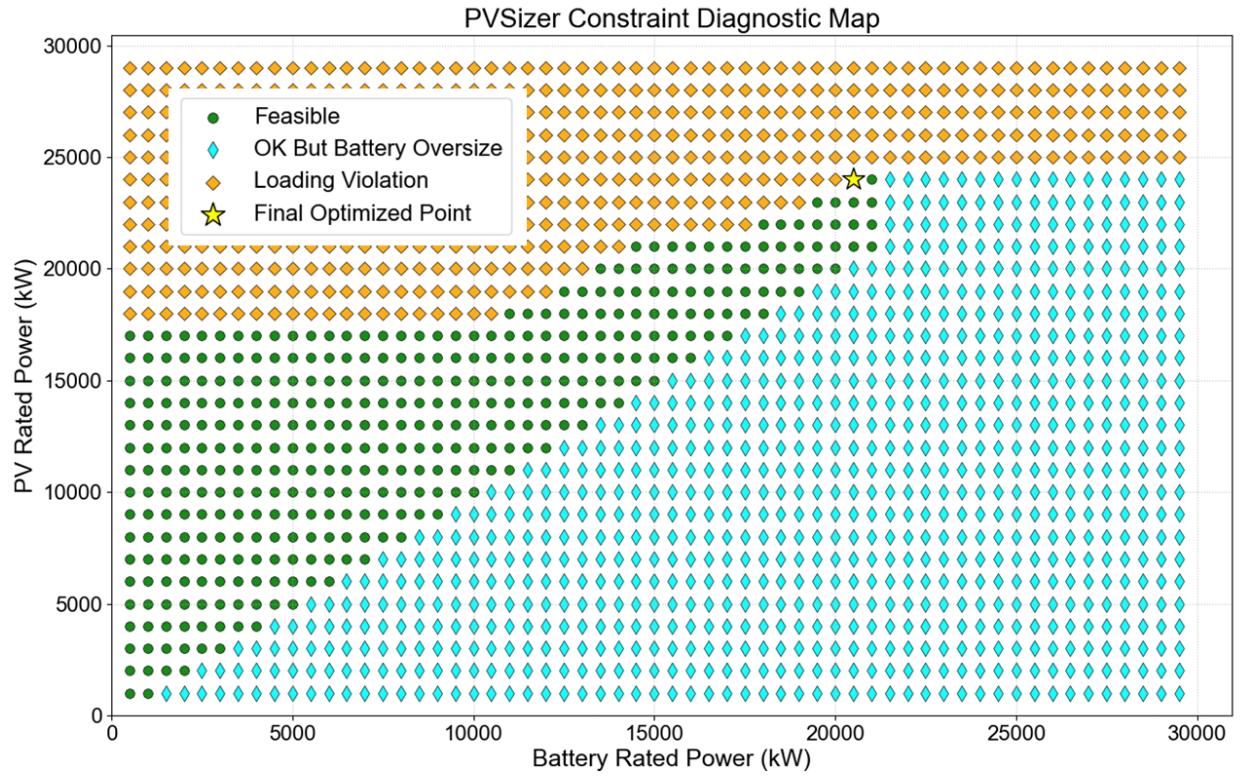


**Figure 1: Traversal/Feasibility map results**

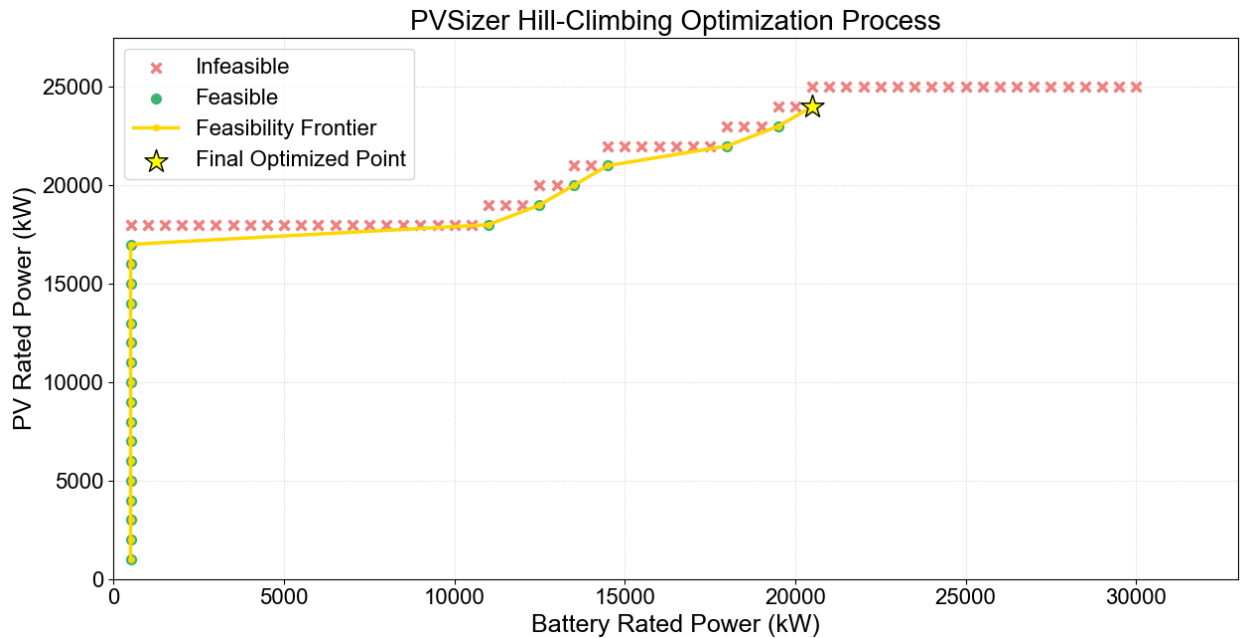


**Figure 2: Quick solution results**

## 6. Measurement-informed Dynamic Aggregation of Distribution Systems

<b>Project Lead:</b> Yilu Liu (UTK), Jin Dong (ORNL)
<b>Graduate Students and Research faculty/associates:</b> Kazi Ishrak Ahmed (UTK), Yuru Wu (ORNL)
<b>Project Duration:</b> 01/2024 – 12/2027
<b>Funding Source:</b> Department of Energy (DOE)

### Summary

With the increasing penetration of distributed energy resources (DERs), such as solar photovoltaics, battery systems, and inverter-based loads, accurately representing their dynamic behavior has become essential for transmission system analysis. However, detailed modeling of distribution-level DERs is often impractical due to data limitations and computational complexity.

This project, led by the UTK and ORNL team as part of the MOON project, develops an aggregated dynamic modeling framework to provide a medium-resolution representation of DER behavior. The approach leverages measurement data to estimate aggregated dynamic parameters, enabling accurate modeling of system responses to disturbances while maintaining computational efficiency.

The model is designed for compatibility with large-scale transmission studies, including WECC 240-bus and utility-scale systems, ensuring practical applicability. By bridging the gap between detailed distribution modeling and transmission-level analysis, this work supports improved stability assessment, situational awareness, and operational decision-making for grid operators.

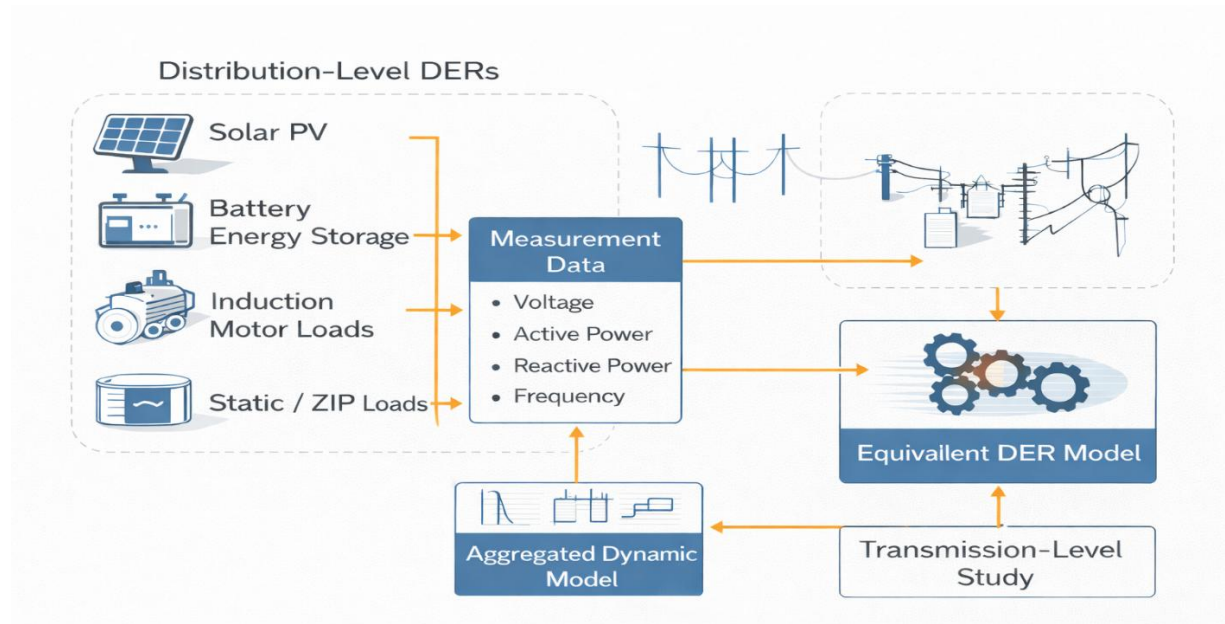


Figure 1: Dynamic Load Modeling Framework

## 7. Acoustic UAV Detection at Electrical Power Substations Using a Harmonic Signature Tracking Method

<b>Project Lead:</b> Yilu Liu(UTK)
<b>Graduate Students and Research faculty/associates:</b> Chong Shen (UTK), Yayu Yang (UTK), Jin Dong (ORNL), Ali Boyaci (ORNL), Ali Ekti (ORNL), Yuru Wu (ORNL)
<b>Project Duration:</b> 11/2025 – 3/2027
<b>Funding Source:</b> DOE

### Summary

The rapid proliferation of unmanned aerial vehicles (UAVs) has introduced increasing security concerns for critical power infrastructure, particularly electrical substations. Unauthorized UAV activities near substations may lead to risks such as equipment surveillance, physical intrusion, and potential disruption of grid operations. Ensuring reliable detection of UAVs in such environments is therefore essential for improving situational awareness and infrastructure protection. To address this challenge, this project develops a robust and practical acoustic-based UAV detection framework, referred to as the Harmonic Signature Tracking Method. This approach leverages the distinctive harmonic sound patterns generated by UAV propellers and provides a cost-effective alternative to more complex sensing modalities.

The proposed method integrates three key components: signal preprocessing, harmonic feature extraction, and temporal voting. First, raw acoustic signals are enhanced using preprocessing techniques such as high-pass filtering and noise reduction to suppress environmental interference and improve signal clarity. Next, the enhanced signal is analyzed in short time windows to identify harmonic structures characteristic of UAV operation. Finally, a temporal voting mechanism is applied to ensure that detected harmonic patterns remain consistent over time, thereby improving detection reliability and reducing false alarms. Unlike machine learning-based approaches, this framework does not require large labeled datasets or computationally intensive training, making it well-suited for real-time implementation and deployment on resource-constrained edge devices.

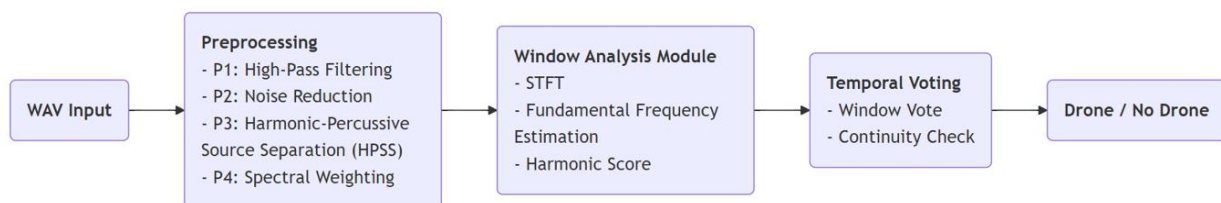


**Figure 1: The architecture**

To evaluate the effectiveness of the proposed approach, a realistic acoustic dataset was constructed under substation-relevant conditions. Due to safety and regulatory constraints, UAV recordings were collected in an open outdoor environment using a DJI Mavic platform at distances ranging from 0 to 50 meters in 5-meter increments, with approximately one minute of data recorded at each distance. In parallel, background noise recordings were obtained near an operational electrical substation to capture representative environmental interference. These datasets were then

combined to preserve realistic propagation characteristics of UAV sounds while incorporating complex substation noise, providing a challenging and practical test scenario for algorithm evaluation.



**Figure 2: Experiment Setup**

Experimental results demonstrate that the proposed method achieves strong detection performance under noisy conditions. Specifically, a low false alarm rate of 4.48% was observed on background-noise-only data, indicating high robustness against non-UAV acoustic interference. Additionally, reliable detection of the DJI Mavic platform was achieved at distances of up to 25 meters. These results highlight the feasibility of using a lightweight, harmonic-based acoustic detection framework for practical UAV monitoring in substation environments. Ongoing work focuses on extending the detection range and further optimizing the system for real-time deployment on edge computing platforms, with the goal of enhancing both the security and operational awareness of modern power systems.

## 8. Development of Load Flexibility Valuation Methodology & Framework to Input into System Planning Tools

<b>Project Lead:</b> Fran Li (UTK)
<b>Graduate Students and Research faculty/associates:</b> Jingzi Liu (UTK), Chenchen Li (UTK)
<b>Project Duration:</b> 10/2023 – 9/2024
<b>Funding Source:</b> Southern Company (SOCO)

### Summary

This project aims to develop a framework for assessing load flexibility and energy sustainability. The primary objective is to accurately predict the potential utilization of flexible loads in the future by analyzing energy load shapes and data related to energy usage. Additionally, this framework aims to facilitate energy savings. Ultimately, the intrinsic value that load flexibility offers to the grid will be adequately captured in this project. In this context, the incentive-based demand response (I-DR) mechanism has gained significant attention by utilizing financial incentives to encourage participation in demand reduction activities on a voluntary basis. Participants can decide whether to reduce load based on accepting or rejecting financial incentives. As such, an I-DR capacity assessment tool is developed to analyze the flexibility of residential loads within the territory of Southern Company (SOCO).

The framework of the I-DR capacity assessment tool is shown in Fig. 1. Given that potential measurement issues may appear in the field data, a data preprocessing module is implemented as the initial step to convert field data into a format suitable for assessment. Subsequently, the core module for I-DR capacity assessment is designed to quantify variations in residential demand behaviors and the corresponding financial incentives required. Finally, to enhance interpretability and decision-making, a visualization module is designed to provide a comprehensive representation of the I-DR potential capacity in the residential service territory, guiding demand elasticity through three-dimensional (3D) figures and statistical lists.

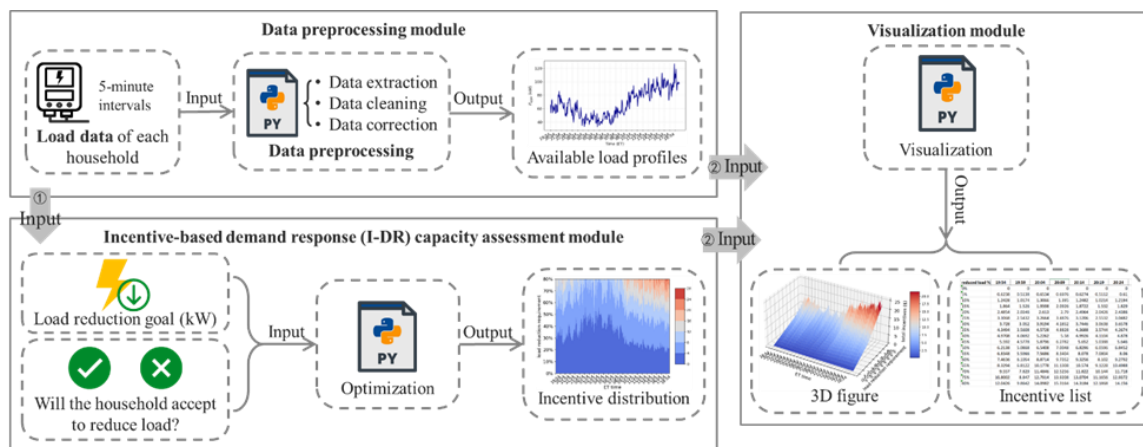


**Figure 1: The framework of I-DR capacity assessment tool**

The first module, the data preprocessing module, comprises a data extraction script to extract discrete field load data, a statistics-based data cleaning method to remove outliers caused by potential measurement issues, and a DNN-based adaptive data correction method to correct identified outliers, ensuring compatibility with subsequent assessments. The second module includes an optimization model designed to minimize the financial incentives paid to households within the service territory for participating in load reduction. The individual energy consumption preferences of each household are incorporated as constraints. After receiving a load reduction goal, households can decide whether to participate in reducing load. Based on their decisions, variable financial incentives are applied to encourage participation. The final module provides a 3D figure to visualize variations in household energy consumption behaviors with the minimum required financial incentives under different timestamps. Additionally, an incentive list is provided to facilitate a straightforward review of specific financial incentives based on the load reduction amount at a given timestamp. Finally, the generated incentive list is formatted as an Excel file. As shown in Fig. 2, SOCO field data from four randomly selected days, one from each season, are used to generate 3D visualization.

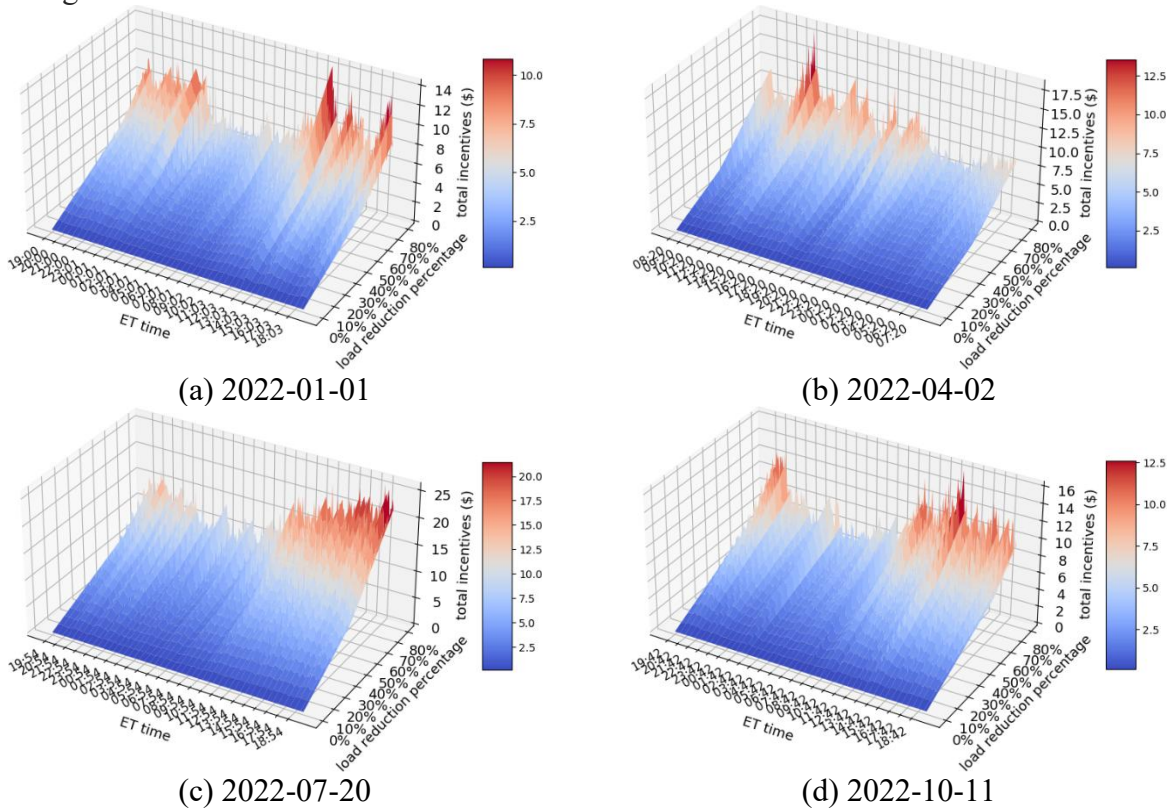


**Figure 2: 3D figures of the total minimum financial incentives required by households within the SOCO service territory to meet load reduction goals**

This tool provides a precise evaluation of the potential for utilizing flexible loads, thereby enhancing the efficient allocation and management of energy resources, which contributes to energy and environmental sustainability. Such residential capacities are instrumental in advancing decarbonization and promoting energy sustainability. Additionally, by quantifying energy elasticity, this tool offers utility companies deeper insights into the regulation of their generation and load, fostering better energy sustainability within the service territory.

## 9. Enhanced Online Oscillation Detection Framework for Sub-Synchronous Oscillation (SSO)

<b>Project Lead:</b> Yilu Liu (UTK)
<b>Graduate Students and Research faculty/associates:</b> Hao Fu (UTK), Yan Wen (UTK), Wenpeng Yu (UTK), Lin Zhu (EPRI)
<b>Project Duration:</b> 11/2025 – 11/2026
<b>Funding Source:</b> EPRI

### Summary

This project presents improvements to the online oscillation detection framework in the Forced Oscillation Localization Tool (FOLT) to support sub-synchronous oscillation (SSO) scenarios. Compared to conventional forced oscillations, SSO events are shorter in duration, higher in sampling rate, and more localized, requiring substantial adaptation of the original detection logic.

To support SSO testing, the data streaming module was updated to handle high-framerate, short-duration datasets and to include frequency measurements alongside voltage and current channels. Early issues with unstable triggering were traced to residual buffered data and timing inconsistencies. These were resolved by introducing explicit timing resets and a quiet initialization period between streaming cycles, significantly improving stability and repeatability.

At the framework level, the original forced-oscillation-oriented detection adapter was modified to better accommodate SSO characteristics. The updated structure strengthens the integration between data streaming, detection, and visualization components, enabling more consistent online detection performance.

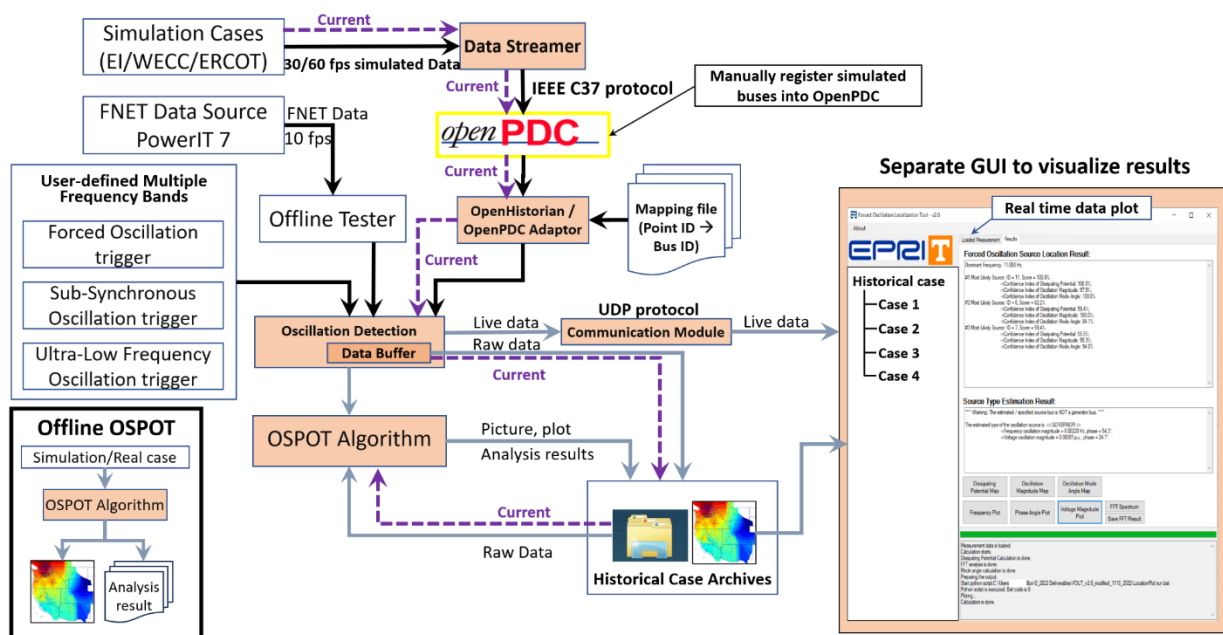


**Figure 1: Updated online oscillation detection framework with SSO-oriented enhancements.**

Detection logic at the individual measurement level was refined to better capture short-lived and localized oscillations. Envelope updating was accelerated, and conservative rejection conditions designed for long-duration events were relaxed. These changes allow the system to detect transient oscillatory behavior without prematurely discarding valid signals.

Frequency-domain processing was also improved to better align with SSO characteristics. Ultra-low-frequency components are excluded, and magnitude-based filtering thresholds were relaxed to preserve weaker oscillatory signatures. These adjustments enhance the reliability of dominant frequency identification and reduce missed detections.

To address the short duration of SSO events, the analysis time window was redefined to align closely with the detected oscillation interval. Early transient portions are excluded, and the window length is reduced to focus on the most informative segment of the signal. This ensures consistency between online detection and offline analysis.

Event lifecycle management was further refined to improve responsiveness. The updated logic enables faster confirmation and termination of oscillation events, reducing unnecessary computation and preventing interference from residual data.

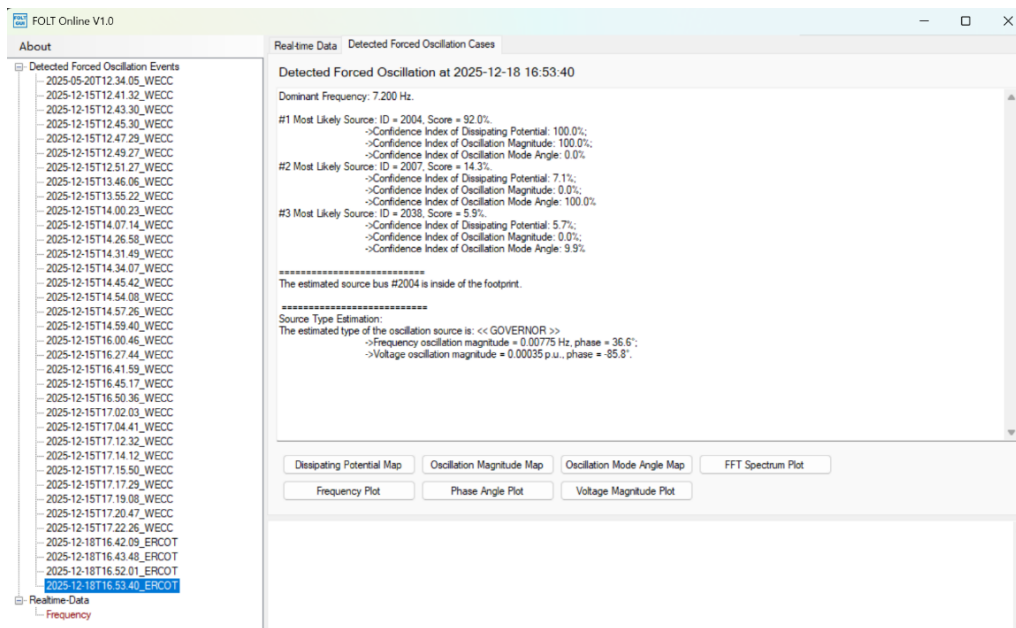


**Figure 3: Example of online GUI output for sub-synchronous oscillation detection.**

Finally, improvements were made to ensure consistency between simulation-based testing and online deployment. These include stricter control of timing, alignment of frame rates, and consistent inclusion of frequency measurements across datasets. Together, these enhancements provide a stable and reliable framework for detecting and analyzing sub-synchronous oscillations in real time.

## 10. Wide-Area Oscillation Damping Control Using FACTS as Actuators: TERNA Case Study

<b>Project Lead:</b> Yilu Liu (UTK)
<b>Graduate Students and Research faculty/associates:</b> Haozong Wang (UTK)
<b>Project Duration:</b> 2/2025 – 12/2025
<b>Funding Source:</b> Terna Energy

### Summary

Low-frequency inter-area oscillations remain an important operational concern in large interconnected power systems, including the European grid. To address this issue, this work investigates a wide-area damping control (WADC) approach that uses phasor measurement unit (PMU) signals as controller inputs and Flexible AC Transmission System (FACTS) devices as actuators. The study focuses on two actuator types: STATCOMs and FACTS resistors. The controller is based on a lead-lag compensation structure, and its effectiveness is evaluated through both simulation studies and field validation. The results indicate that both actuator types are capable of providing effective oscillation damping in practical transmission-system applications.

The developed WADC framework employs the sophisticated lead-lag compensation control and then adapted to different actuator technologies, as shown in Figure 1. For STATCOM, the actuator is represented in PSS®E using the CSTCNT model, and the damping control command is injected into the voltage-reference setpoint. For FACTS resistor, the actuator is represented using REGCA1 and REECDU1 models, and the damping command can be applied through active-power and reactive-power references separately or simultaneously.

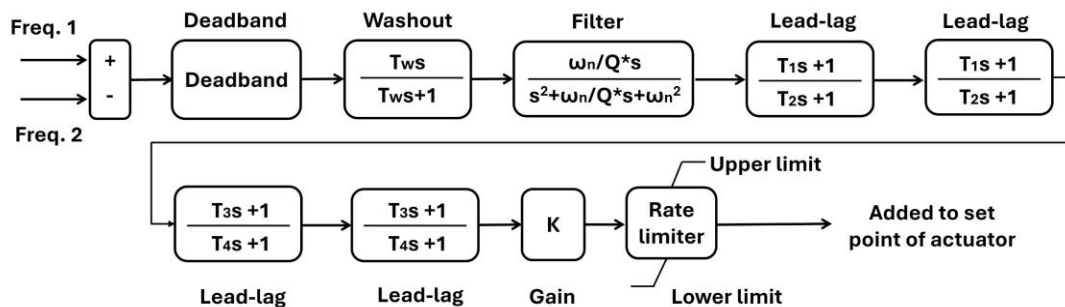
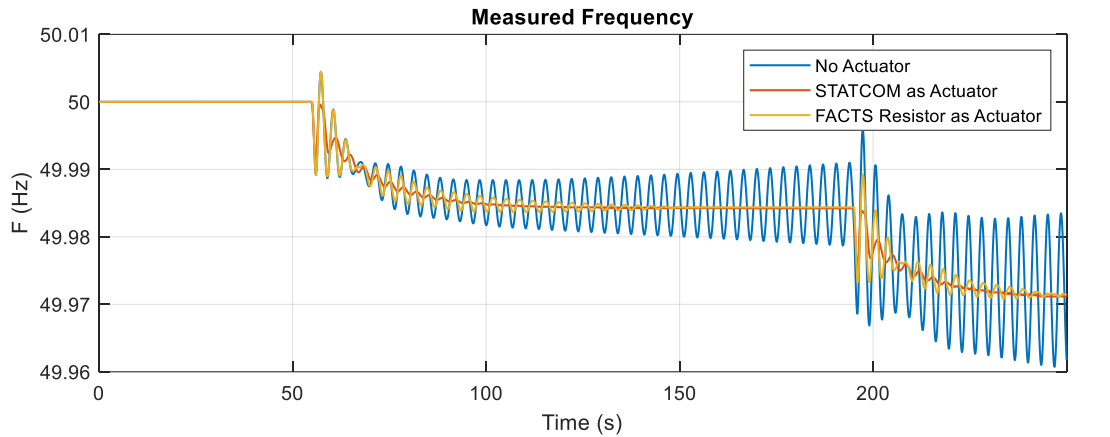


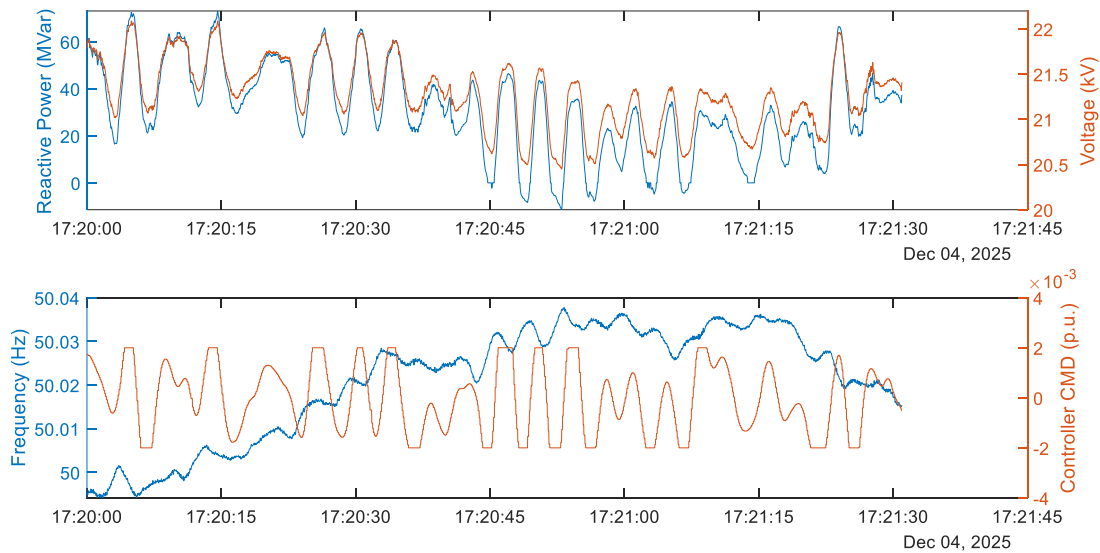
**Figure 1: Controller Diagram**

A broad set of simulation studies was conducted to assess the influence of actuator capacity, installation location, number of devices, available control margin, and operational constraints. For FACTS resistors, the comparison also included different control channels, especially active-power and reactive-power modulation. The simulation results show that both STATCOMs and FACTS resistors are feasible WADC actuators, and that increasing total actuator capacity generally improves damping performance. Among the tested FACTS resistor control strategies, active-power control typically provides better damping performance than reactive-power control in the

studied scenarios. In contrast, actuator location has a relatively smaller influence on the overall damping effectiveness. The results also highlight that practical deployment constraints, such as output saturation and ramp-rate limits, must be considered when designing and tuning wide-area damping controllers. Field validation further confirms the practicality of the proposed approach. For STATCOM-based damping control, both open-loop and closed-loop tests were carried out, and the closed-loop test demonstrated measurable improvement in oscillation damping. In particular, the damping ratio of a 0.28 Hz mode increased from 7% to 9%, verifying that STATCOMs can effectively serve as actuators for wide-area oscillation damping in a real grid environment. The representative results of simulations and field tests are shown in Figure 2.



(a) Representative Simulation Results



(b) Closed-Loop Field Test Results

**Figure 2: Representative Results of WADC using FACTS as Actuators**

This study shows that both STATCOMs and FACTS resistors are promising actuator candidates for PMU-based WADC. While STATCOM field tests have already demonstrated the concept, field testing of FACTS resistors is expected in the next phase, which will further validate their practical applicability and provide additional guidance for large-scale deployment

## 11. Frequency Response of Windowed DFT Phasor Estimation: Impact on Oscillation Observability

<p><b>Project Lead:</b> Yilu Liu (UTK / ORNL)</p> <p><b>Graduate Students and Research faculty/associates:</b> Jiahui Yang (UTK), Yuru Wu (UTK/ORNL), Haozong Wang (UTK), Yu Liu (UTK), Biao Sun (UTK), Clifton Black (Southern Company Services)</p>
<p><b>Project Duration:</b> 2026.1-now</p>
<p><b>Funding Source:</b> UTK</p>

### Summary

The growing penetration of inverter-based resources (IBRs) in modern power systems has introduced sub-synchronous oscillations spanning 0.1–30 Hz, which can degrade equipment and, in severe cases, precipitate system-wide blackouts. Phasor Measurement Units (PMUs) are widely deployed for oscillation monitoring, and most PMU outputs are produced through windowed Discrete Fourier Transform (DFT) based phasor estimation. The window length required by IEEE Standard C37.118.1—short for P-class, long for M-class—fundamentally shapes the frequency response of the estimator and, consequently, how faithfully oscillation components are preserved in the reported phasor stream. Under certain conditions, these windowing effects can distort reported oscillation magnitude and phase, or suppress oscillation components entirely, yielding PMU data that appears quiescent even when the underlying grid is actively oscillating.

This project derives the complete complex-valued frequency response of the windowed DFT phasor estimator under both magnitude and phase modulation of the input signal. The two modulation models are:

$$x[p] = \sqrt{2}V_{\text{rms}}(1 + \alpha \sin(\Omega_m p + \varphi_m)) \cos(\omega_0 p + \varphi_0) \quad (1)$$

$$x[p] = \sqrt{2}V_{\text{rms}} \cos(\omega_0 p + \varphi_0 + \beta \sin(\Omega_m p + \varphi_m)) \quad (2)$$

Propagating each through an L-point windowed DFT yields closed-form expressions for the resulting phasor. The analytical result is the frequency-dependent complex gain

$$H_1(e^{j\lambda}) = \frac{\sqrt{2}}{L} e^{j\lambda(L-1)/2} \cdot \frac{\sin(L\lambda/2)}{\sin(\lambda/2)} \quad (3)$$

whose magnitude and phase,

$$G = |H_1(e^{j\Omega_m})|, \quad \theta = \angle H_1(e^{j\Omega_m}) \quad (4)$$

govern the attenuation and phase shift imposed on any oscillation component. Because this gain is known in closed form, the true oscillation amplitude and phase can be recovered from measured PMU data using

$$A_{\text{rec}} = \sqrt{2} \cdot \frac{A_{\text{meas}}}{G}, \quad \varphi_{\text{rec}} = \varphi_{\text{meas}} - \theta \quad (5)$$

provided the oscillation frequency does not coincide with a comb-null of the response. The magnitude and phase of the complex gain are plotted in Figure 1 for window lengths parameterized by  $h = 1, 2, 4, 8$  (corresponding to increasingly long DFT windows).

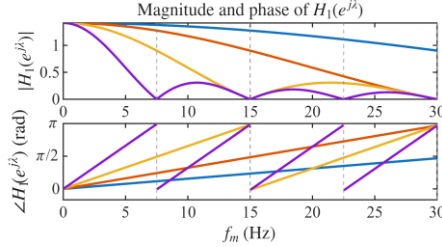


Figure 1: Magnitude and phase of the complex gain  $H_1$

Figure 2 presents the time-domain case study that validates the analytical model. Synthetic signals with magnitude modulation ( $\alpha = 0.010$ ) or phase modulation ( $\beta = 0.020$  rad) at controlled modulation frequencies are passed through the windowed DFT phasor estimator, and the  $V_{\text{mag}}$  and  $V_{\text{ang}}$  streams are calculated for  $h = 1, 2, 4, 8$ . Subfigure (a) — a slow 0.1 Hz magnitude modulation — shows all four window lengths producing nearly overlapping  $\pm 1\%$  envelopes with negligible attenuation, confirming that low-frequency oscillations are preserved regardless of PMU class. Subfigure (b), magnitude modulation at  $f_m = 15$  Hz, is the critical comb-null case: the analytical gain  $G$  predicts exact zeros for  $h = 4$  and  $h = 8$ , and the  $h = 4$  and  $h = 8$  traces collapse to a flat 1.0 RMS line in the plot, completely suppressing a real oscillation that is still present in the input. Only the  $h = 1$  and  $h = 2$  traces retain visible oscillation, though already attenuated relative to the true  $\pm 1\%$  amplitude. Subfigure (c), magnitude modulation at  $f_m = 20$  Hz, exhibits the progressive-attenuation regime: the  $h = 1$  trace reproduces the full  $\pm 1\%$  amplitude,  $h = 2$  shows moderate attenuation,  $h = 4$  is noticeably smaller, and  $h = 8$  is reduced to roughly one-tenth of the true amplitude — a quantitative match to the  $G$  values read from Figure 1 at 20 Hz. Subfigure (d), phase modulation at the same  $f_m = 20$  Hz, shows the identical attenuation pattern in  $V_{\text{ang}}$  together with clearly offset zero-crossings between the four  $h$  values, confirming the analytically predicted phase shift  $\theta$ . Together the four cases demonstrate that (5) yields faithful calculation of both amplitude and phase whenever  $f_m$  avoids a comb-null.

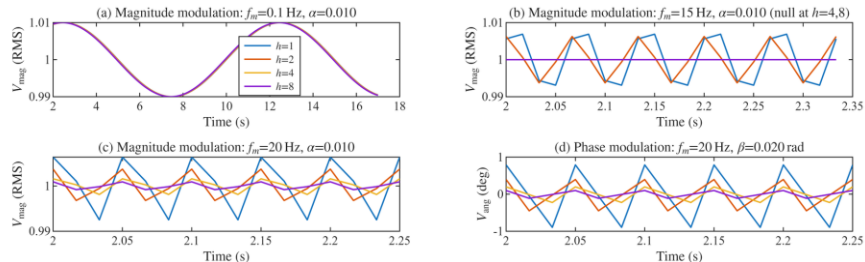


Figure 2: Time-domain case study of reconstructed phasors for  $h = 1, 2, 4, 8$ . (a) Magnitude modulation at  $f_m = 0.1$  Hz; (b) magnitude modulation at  $f_m = 15$  Hz (comb-null at  $h = 4, 8$ ); (c) magnitude modulation at  $f_m = 20$  Hz; (d) phase modulation at  $f_m = 20$  Hz.

The practical implications for utility oscillation monitoring are significant. The windowed DFT introduces both frequency-dependent magnitude attenuation and phase shift to oscillation

components, so detected oscillation magnitudes may systematically underestimate true severity, and the absence of oscillations in phasor data does not guarantee oscillation-free operation—oscillations may be canceled at comb-null frequencies or heavily attenuated well below detection thresholds. For sub-synchronous oscillation monitoring driven by IBR proliferation, shorter DFT windows (P-class configurations) are preferable because they push comb-nulls well outside the frequency band of interest and flatten the passband; an anti-aliasing filter upstream of the estimator is additionally recommended to suppress image components. Beyond monitoring, the recovery formula (5) enables direct reconstruction of true oscillation amplitude and phase from existing PMU archives whenever  $f_m$  is known or can be identified via spectral analysis.

## 12. OEDI – Solar Grid Integration Data and Analytics Library

<b>Project Lead:</b> Yilu Liu (UTK)
<b>Graduate Students and Research faculty/associates:</b> Yayu Yang (UTK), Haozong Wang (UTK), Hao Fu (UTK), Zhengfa Zhang (UTK), Jin Dong (ORNL), Boming Liu (ORNL)
<b>Project Duration:</b> 9/2021 – 9/2026
<b>Funding Source:</b> DOE

### Summary

As the integration of distributed energy resources (DERs) into distribution systems accelerates, existing models are increasingly unable to meet emerging R&D needs due to proprietary constraints, limited data quality, and the absence of high-DER scenarios, time-series data, and transient representations. Moreover, the lack of standardized tools for algorithm testing and benchmarking restricts reproducibility and hinders practical adoption. At the same time, the growing penetration of EVs, energy storage, and flexible loads introduces faster system dynamics and greater operational complexity, demanding more advanced modeling and analytical capabilities.

This project aims to develop an open-source distribution system modeling and data platform tailored for high solar penetration. The main tasks include: (1) developing representative models with high DER integration and enriched datasets; (2) enabling key use cases such as demand-side management and dynamic EV charging through modular data processing frameworks; (3) establishing open interfaces and benchmarking tools to support algorithm validation and comparison; and (4) creating a transient event library and associated analysis tools to capture critical phenomena such as faults, harmonics, and oscillations.

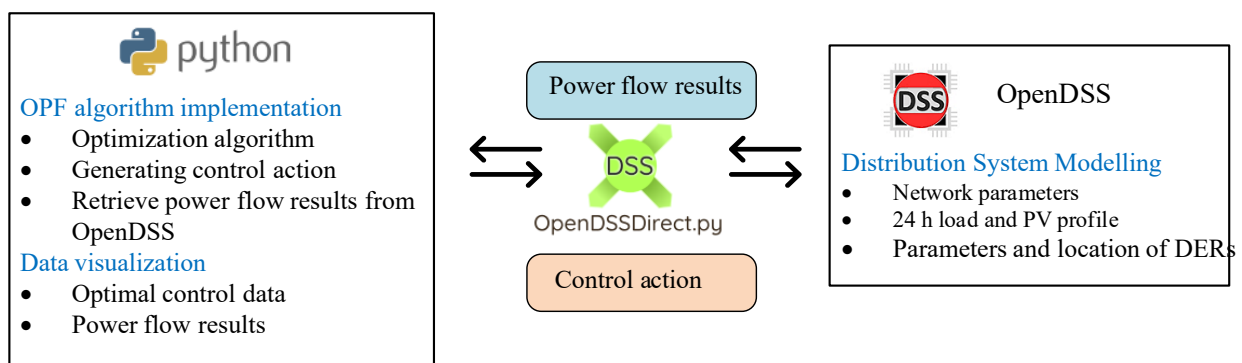


**Figure 1: Hybrid D-OPF Framework**

### 13. Real-Time Local Damping of Wideband Power Oscillations Using Droop-Controlled IBRs

<b>Project Lead:</b> Yilu Liu (UTK)
<b>Graduate Students and Research faculty/associates:</b> Saurav Dulal (UTK)
<b>Project Duration:</b> 10/2025-10/2026
<b>Funding Source:</b> ORNL/DOE

#### Summary

This project develops a real-time local damping strategy for inverter-based resources (IBRs) to mitigate wideband power oscillations in modern power systems. As IBR deployment increases, oscillatory modes can vary in frequency, severity, and location, while conventional power oscillation damping schemes often rely on fixed tuning or centralized coordination. The proposed approach instead uses the fast-response capability of droop-controlled IBRs to provide decentralized damping based on local measurements. By activating only when sustained oscillations are detected and by adapting control parameters online, the framework is intended to improve responsiveness, scalability, and practical deployability in inverter-dominated grids.

The control architecture, shown in Fig. 1, combines local measurement and buffering, continuous modal analysis, envelope-based triggering, phase compensation, and mode-aware droop control. Frequency deviations measured at the IBR terminal are stored in a rolling window and processed using a modal analysis method such as fast Fourier transform to identify the dominant oscillation mode. Once the oscillation envelope exceeds a predefined threshold, the controller computes phase compensation parameters  $T1$  and  $T2$  and assigns a gain  $K$  according to the detected mode characteristics, for example using a residue-based gain selection strategy. This enables rapid delivery of an appropriately phased damping signal through active or reactive power modulation.

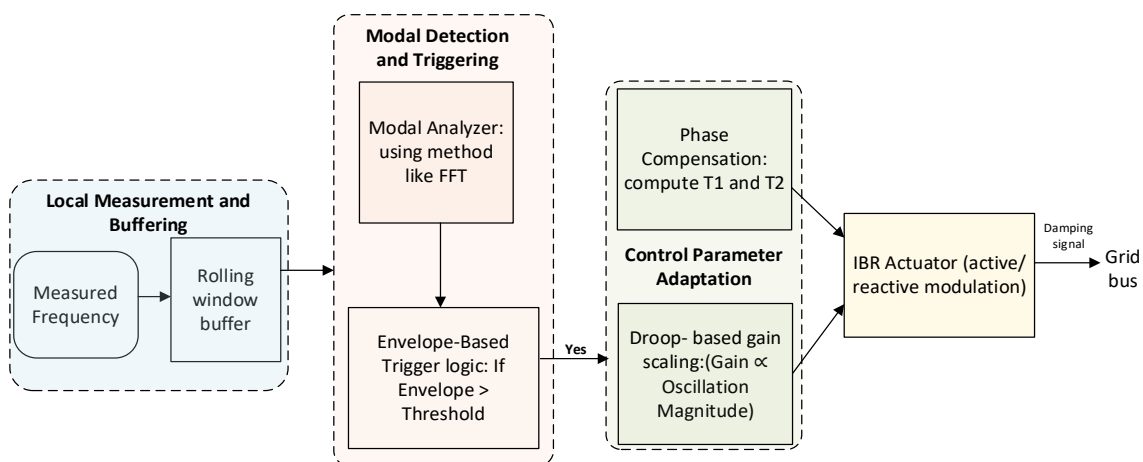


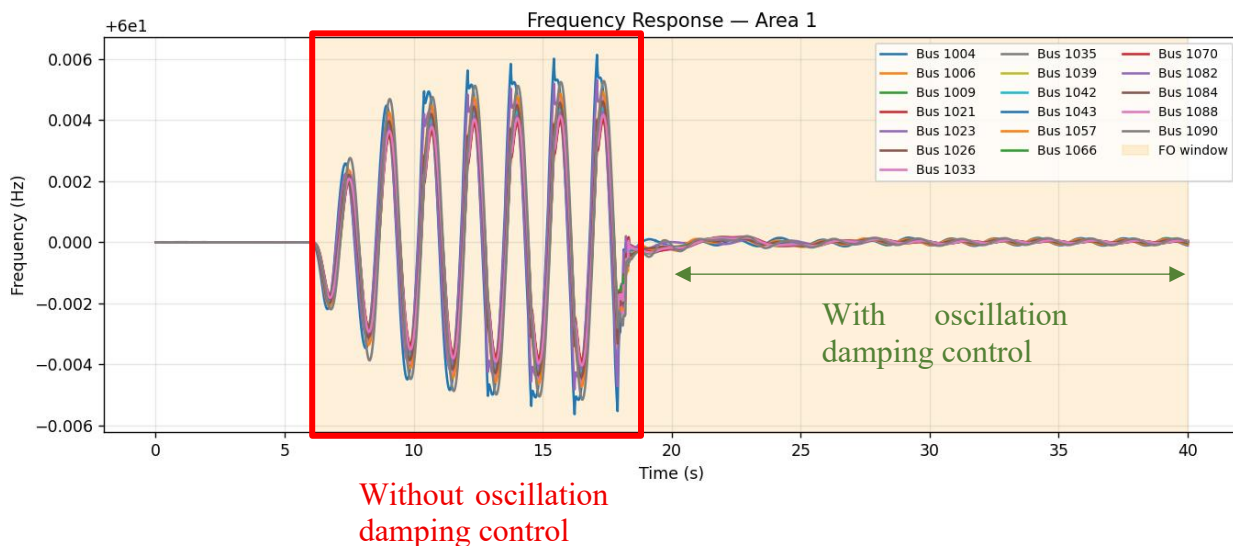
**Figure 1: Real-time local control architecture with envelope-based triggering and mode-aware droop-modulated damping via IBRs.**

Implementation is envisioned in the ERCOT synthetic power system using Python and PSS/E co-simulation. Small-signal oscillations can be introduced through low-amplitude sinusoidal perturbations at generator mechanical power or external signal functions, allowing the controller to be evaluated across a broad oscillation range. Because measurement, detection, and gain adaptation are performed locally, the framework can be deployed in a modular manner across multiple IBRs without requiring centralized coordination. This structure also supports continuous background updating so that control action can be applied with minimal latency once a trigger condition is satisfied.

Compared with conventional IBR-based damping schemes tuned for fixed modes, the proposed framework is designed to deliver frequency-aware and severity-aware damping over a wide operating band. The project therefore establishes a practical foundation for adaptive oscillation mitigation in future low-inertia systems, with potential benefits for small-signal stability, operational flexibility, and scalable integration of inverter-based controls. The resulting methodology can support subsequent testing, controller tuning, and broader evaluation of decentralized damping strategies in realistic transmission system environments. A preliminary conceptual result is as shown in Fig. 2.

Table 1: Summary of the proposed adaptive damping workflow

Module	Role in the framework
Local measurement and buffering	Collect local frequency deviations and maintain a rolling data window for real-time analysis.
Modal detection and triggering	Use FFT-based spectral analysis and envelope logic to identify sustained oscillations and activate control only when needed.
Control adaptation parameter	Compute phase compensation terms T1 and T2 and assign a mode-aware gain K based on the detected oscillation characteristics.
IBR actuation	Inject active or reactive power modulation through the IBR interface to provide appropriately phased damping.



## 14. Large-Scale Data Center Load Modeling With Real Event Scenario

<b>Project Lead:</b> Dr. Yilu Liu (UTK), Amirreza Sahami (Dominion Energy)
<b>Graduate Students and Research faculty/associates:</b> Stephanie Tomasik (UTK), Xinlan Jia (UTK)
<b>Project Duration:</b> 2024 – Present
<b>Funding Source:</b> Dominion Energy

### Summary

This project investigates how large-scale data center loads can be more accurately represented in bulk power system dynamic simulations. As data center development accelerates across the United States, these loads are becoming large enough to noticeably affect voltage and frequency behavior during major disturbances. Conventional static load representations are often not sufficient to capture the fast and voltage-sensitive response of data center loads. The goal of this work is to improve how these emerging loads are modeled so planners can better evaluate their impact on system reliability and stability.

To address this need, the project applies the composite load model (CMLD) in PSS®E to represent large-scale data center behavior in an Eastern Interconnection planning case. A real disturbance event from July 10, 2024, involving a permanent 230 kV line fault, followed by six reclosing attempts, and the transfer of approximately 1,500 MW of voltage-sensitive load, was used as the primary study scenario. Dynamic simulations were performed to examine voltage and frequency responses at key buses and load areas, and the model behavior was compared with observed system performance. This approach allows the study to evaluate whether existing composite load modeling methods can reasonably reproduce the disconnection and reconnection characteristics of large data center loads during severe system events.

Initial results show that the composite load model provides a useful framework for representing aggregate data center behavior, but also reveal limitations in matching the full ride-through and recovery characteristics seen in actual events. The study emphasizes the importance of load composition, protection settings, and voltage sensitivity in determining the system response. These findings support continued refinement of data center load modeling and provide a foundation for future work on improved parameterization and alternative model structures. This project contributes to ongoing efforts to better represent emerging large electronic loads in planning studies and to strengthen grid resilience as data center penetration continues to grow.

# Composite Load Model

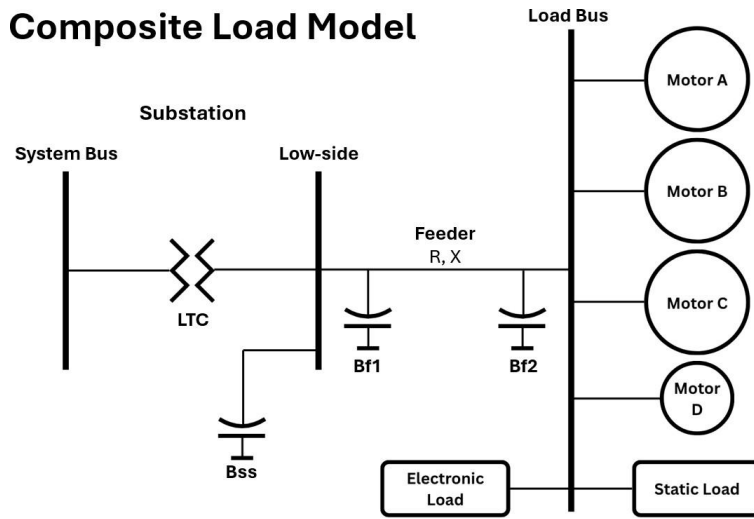


Figure 1: Visual representation of CMLD model developed by WECC.

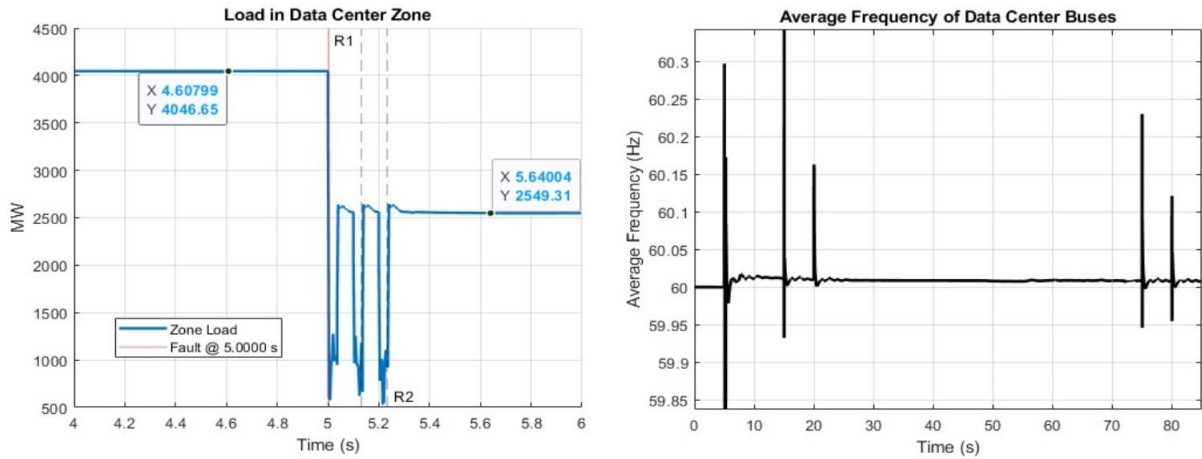


Figure 2: Load and frequency response from event simulation for the data center zone.

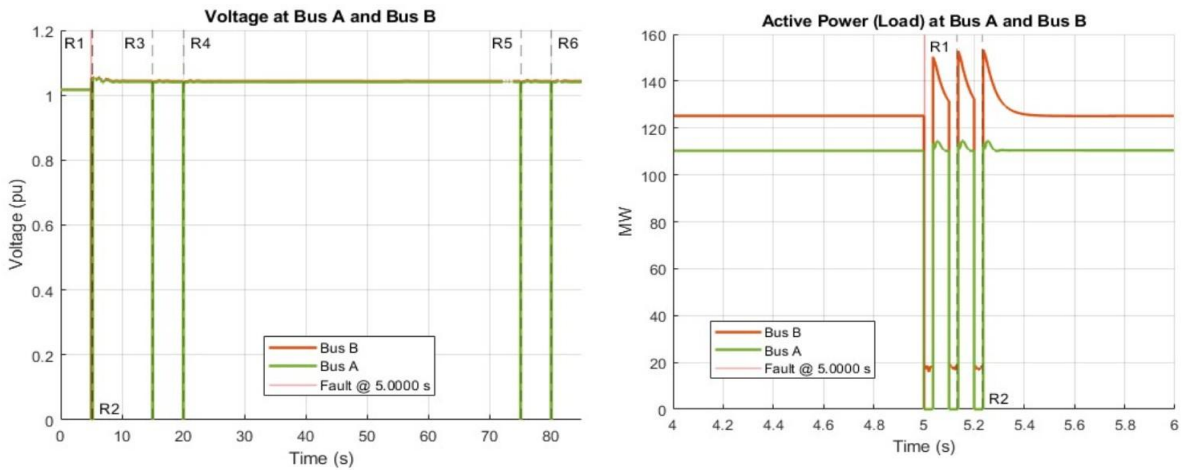


Figure 3: Voltage and load response from event simulation for the buses on either side of the line fault.

## 15. Detection of Large Load Loss Event: Focus on the Northern Virginia Data Center Hub

**Project Lead:** Yilu Liu (UTK)

**Graduate Students and Research faculty/associates:** Qian Liu (UTK)

**Project Duration:** 10/2024 – 2026

**Funding Source:** National Science Foundation

### Summary

A phase-to-ground fault on a 230 kV transmission line in Northern Virginia’s Loudoun County on July 10, 2024, led to the transfer of about 1,500 MW of data center load to backup diesel generators. Voltage profile observations suggest that many large load facilities-initiated load transfer when local voltage dropped below a critical threshold.

This finding guided the deployment of additional monitoring units in the area, which subsequently captured multiple similar load-trip events over the following year, further confirming the strong association between large load-loss events and data center operations in the Loudoun County corridor.

By extending the FDR units deployment surround by Loudoun County data center farm, we’re able to capture more events starting from 2025. And most of the cases appear to be data center detecting a single voltage dip, and they initiate drop in load profile but recover gradually.

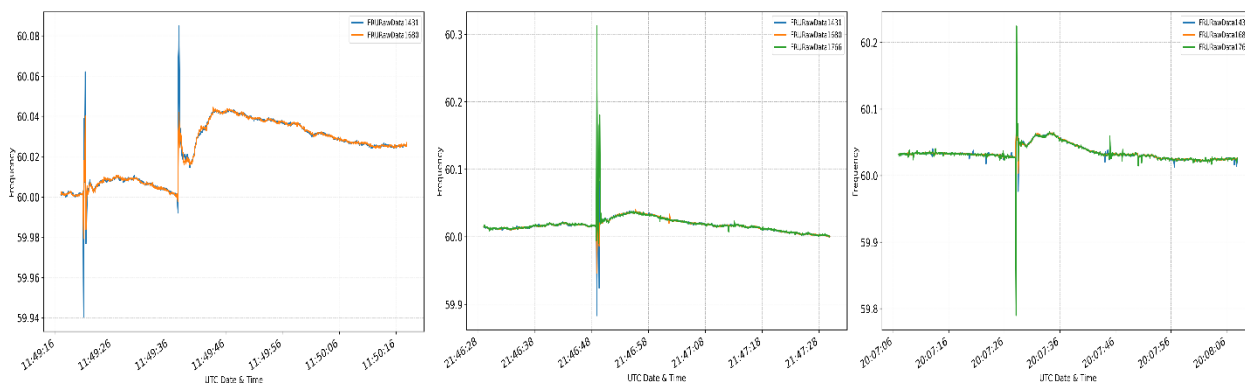


**Figure 1: Data Center Load Loss Events in 2025**

## 16. Bridging PMU Measurements and Dynamic Simulation for Oscillation Analysis

**Project Lead:** Yilu Liu (UTK)

**Graduate Students and Research faculty/associates:** Qian Liu (UTK)

**Project Duration:** 2/2025 – 2026

**Funding Source:** Florida Power Light

### Summary

Low-frequency oscillations continue to challenge large power systems, making persistent mode identification essential for effective monitoring and control. Using long-term FNET/GridEye measurements, this paper combines ARMA-based ambient modal estimation and oscillation event analysis with large-scale PSS®E simulation to identify and validate dominant modes in the Eastern Interconnection, especially in Florida. The proposed workflow connects field measurements with dynamic simulation and supports improved understanding of oscillatory behavior and future damping control design.

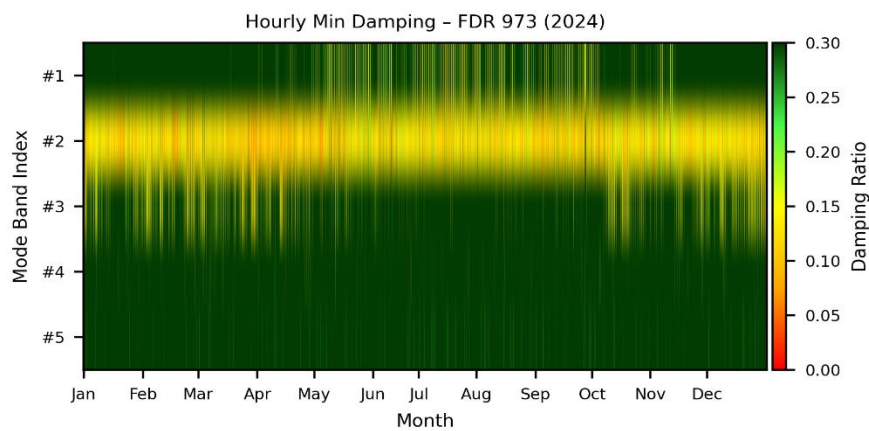


**Figure 1: Hourly Damping by Mode**

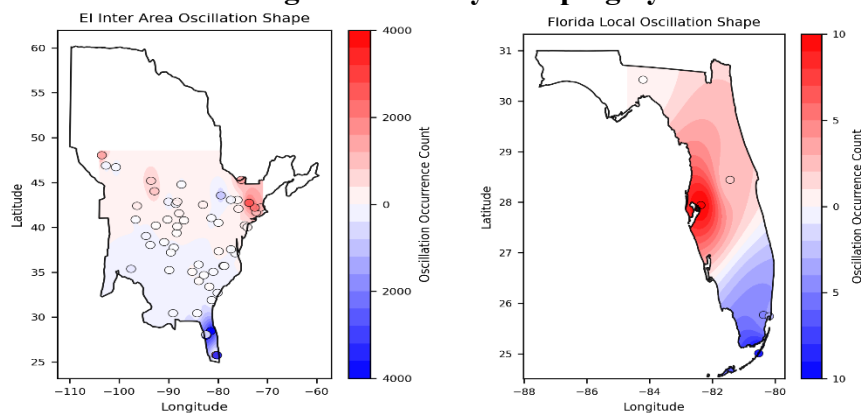


**Figure 2 : Mode Spatial Shape by Event Occurrence**

ARMA-based modal estimation is applied to ambient frequency data using a 20-minute window. Fitting an ARMA model to each window, modal frequency and damping can be extracted, allowing weakly damped oscillation modes to be identified under normal operating conditions.

PSS®E dynamic simulations were performed for 10 contingencies under spring, summer, and winter operating cases to evaluate the oscillatory response and compare seasonal modal behavior.

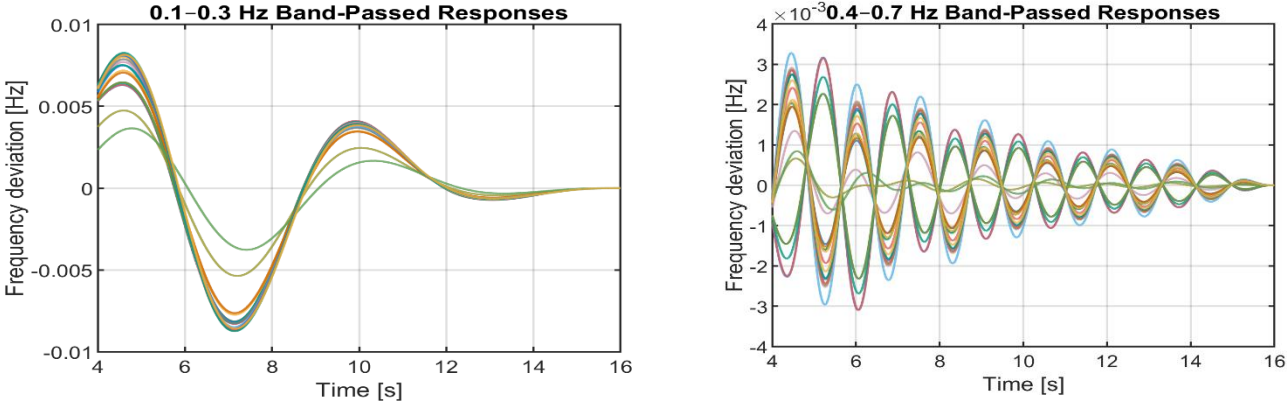


**Figure 3 Frequency after Bandpass**

## 17. A Heterogeneous Multiscale Method for Efficient Simulation of Power Systems with Inverter-Based Resources

<b>Project Lead:</b> Kai Sun (UTK)
<b>Graduate Students and Research faculty/associates:</b> Kaiyang Huang (UTK)
<b>Project Duration:</b> 03/2024 – 02/2027
<b>Funding Source:</b> National Science Foundation (NSF)

### Summary

This project presents a novel simulation framework for power systems with high penetration of inverter-based resources (IBRs), where system dynamics span multiple timescales ranging from microsecond-level electromagnetic transients (EMT) to slower electromechanical responses. Such multi-timescale behavior leads to highly stiff nonlinear models, making conventional time-domain simulations computationally expensive due to the requirement of extremely small-time steps for numerical stability. Existing approaches, including co-simulation and offline model reduction, often suffer from interface inconsistencies, reduced accuracy, and difficulty in defining appropriate system partitions. To address these challenges, this work proposes a Heterogeneous Multiscale Method (HMM)-based framework that enables efficient and accurate simulation directly on full EMT models without requiring explicit model reduction.

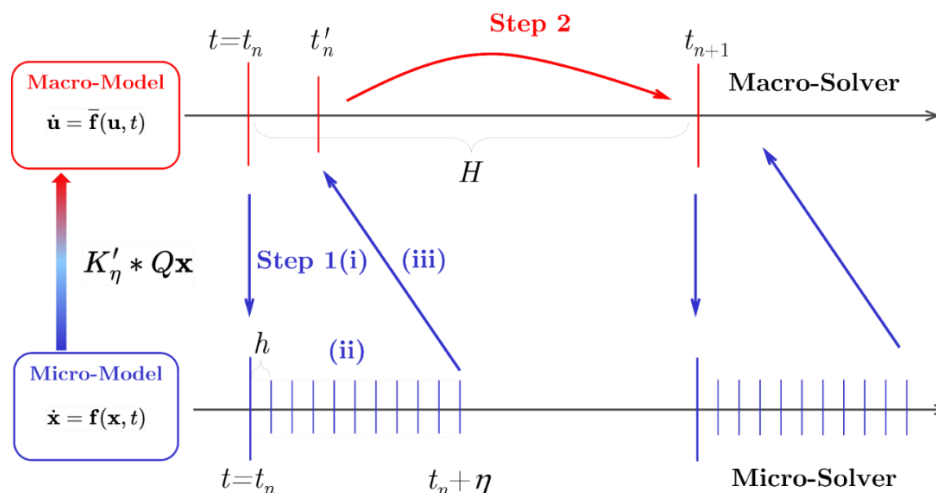


**Figure 1: A two-timescale HMM scheme.**

The core idea of the proposed method is to alternate between two complementary processes: a micro-process that resolves detailed EMT dynamics and a macro-process that advances slower system dynamics using significantly larger time steps. As illustrated in Fig. 1, the framework repeatedly performs short bursts of detailed micro-simulations over a small time interval to extract essential system behavior, followed by long macro-steps that evolve the system efficiently. Instead of constructing an explicit reduced-order model, the method estimates macroscopic dynamics on the fly using a kernel-based averaging technique applied to the micro-state trajectories. This allows the framework to adapt to system conditions dynamically while preserving both fast and slow dynamics of interest.

A key contribution of this work is the introduction of transformation operators that link micro-state variables to macro-state representations. These operators enable seamless transitions between the two processes without loss of accuracy. In addition, the framework incorporates a semi-analytical Differential Transformation (DT) method as the micro-solver, allowing variable-step simulation with explicit error control. The macro-process further employs adaptive step-size control to balance computational efficiency and numerical accuracy. Theoretical analysis establishes bounds on the estimation error and provides insights into the relationship between step sizes, kernel parameters, and achievable speedup, demonstrating that significant acceleration can be achieved while maintaining controlled accuracy.

The overall workflow of the proposed approach is summarized in Fig. 2, where the simulation dynamically switches between micro- and macro-processes depending on system conditions. During fast transients such as faults, the method relies on detailed EMT simulation to accurately capture high-frequency dynamics. Once these fast dynamics decay, the algorithm transitions to macro-processes with enlarged time steps, significantly reducing computational cost while maintaining accuracy for slower dynamics.

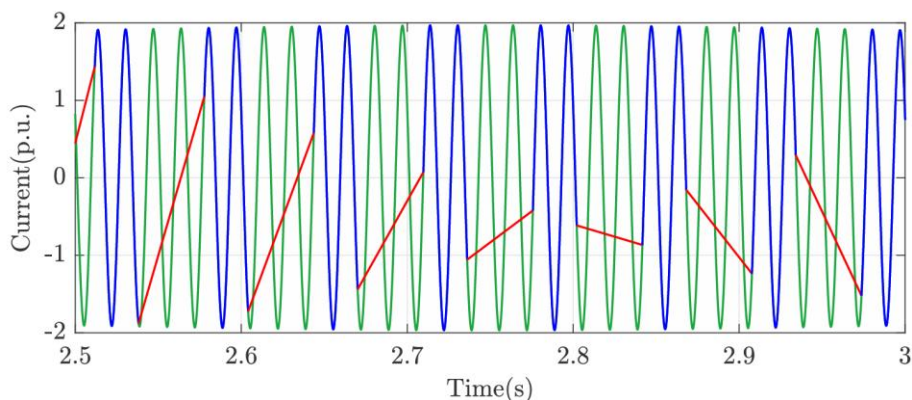


**Figure 2: Simulation results for 390 bus system: Phase A current of the branch line 1-2.**

The effectiveness and scalability of the proposed method are validated through case studies on a two-area system, the IEEE 39-bus system, and a large-scale 390-bus system. Simulation results show that the method accurately reproduces both fast transient responses and long-term dynamics, with substantial reductions in computational time compared to traditional EMT solvers. In particular, the method achieves several-fold speedup in medium-scale systems and up to tens-of-times acceleration in large-scale simulations, while maintaining comparable accuracy to benchmark solutions.

Overall, the proposed HMM-based framework provides a unified and adaptive approach for multi-timescale power system simulation. By eliminating the need for explicit model reduction and enabling dynamic switching between timescales, it offers a scalable and robust solution for analyzing modern power systems with high IBR penetration. The framework is general and can be extended to incorporate additional timescales and more detailed device-level dynamics in future work.

## 18. PowerCascade: Power Systems Cascading Failure Analysis Synthetic Dataset

<b>Project Lead:</b> Kai Sun (UTK)
<b>Graduate Students and Research faculty/associates:</b> Tingwei Chen (UTK), Zhenping Guo (UTK), Kaiyang Huang (UTK)
<b>Project Duration:</b> 06/2025 – 08/2025
<b>Funding Source:</b> National Science Foundation (NSF)

### Summary

The stability and reliability of power systems are critical concerns in modern energy infrastructure. As the power grid becomes increasingly complex due to the integration of renewables and distributed energy resources, the risk of cascading failures—sequential outages triggered by an initial fault—has grown substantially. Without timely intervention, these cascading events can escalate into widespread blackouts affecting millions of people, as evidenced by major incidents including the 2012 India blackout (affecting over 600 million), the 2019 Argentina–Uruguay–Paraguay blackout (48 million), and the 2011 Southwest U.S. event (2.7 million). Despite the severity of these events, the research community has lacked a standardized, high-quality dataset for developing and benchmarking AI-based methods for cascading failure analysis. This project introduces PowerCascade, a synthetic dataset specifically designed to support research on the application of artificial intelligence (AI) for learning and predicting the propagation of cascading failures in power systems.

The PowerCascade dataset is generated using an emulation framework inspired by the Oak Ridge–Pserc–Alaska (OPA) model and implemented in both MATLAB. The Northeast Power Coordinating Council (NPCC) 140-bus test system—comprising 140 buses and 233 transmission lines—serves as the testbed. Cascading failures are initiated by N-2 contingency events, i.e., the simultaneous outage of two transmission lines, representing the starting point of each simulation. The data generation workflow is illustrated in Fig. 1. For each simulation, the system is initialized with pre-fault conditions (bus voltage levels and active power injections) randomly sampled within a predefined range to ensure diversity across scenarios. The DC optimal power flow (OPF) model is then applied to re-dispatch generation following each fault, and overloaded lines are tripped to simulate system protection actions. This iterative process continues until no further failures occur, capturing the full cascade evolution. To comprehensively represent real-world operating conditions, emulation is conducted under three load scenarios: light load ( $0.8\times$  base), normal load ( $1.0\times$  base), and heavy load ( $1.2\times$  base).

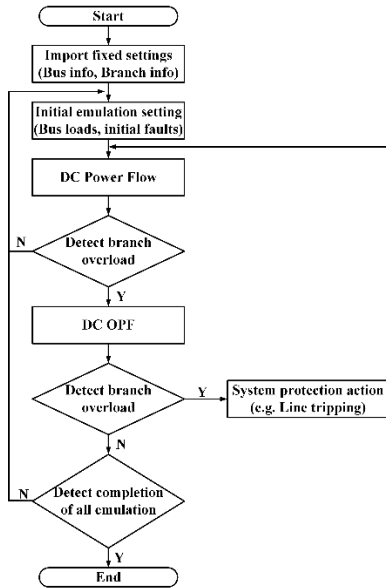


**Figure 1:** Data generation workflow of the PowerCascade dataset

The dataset is organized into two components: static parameters (Buses.csv and Branches.csv) capturing topology, impedances, and capacity limits; and dynamic failure records documenting branch outage sequences and bus load values across stages, in four CSV files by load condition plus a consolidated FailureData\_All.csv. As shown in Fig. 2, the dataset contains 13,500 scenarios and 28,811 data entries in total.

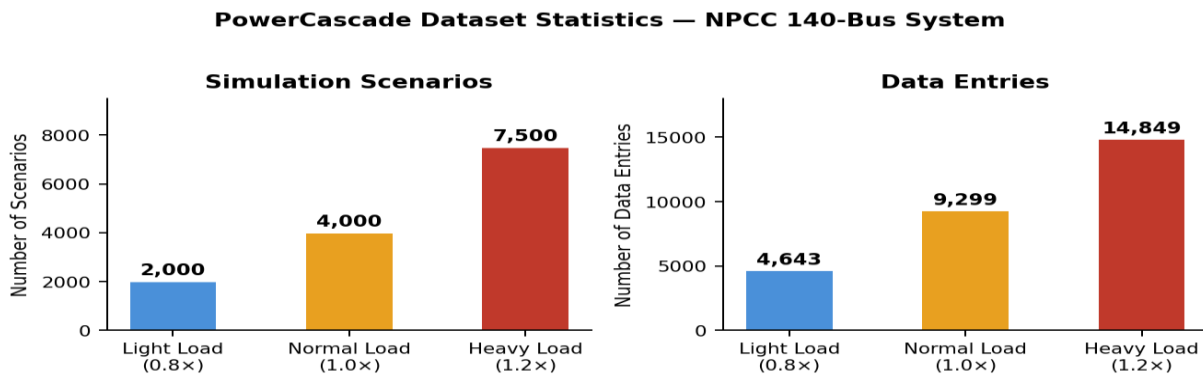


**Figure 2:** Dataset statistics across three load conditions: (a) simulation scenarios and (b) data entries

PowerCascade serves multiple research purposes. In power engineering, it enables AI-based failure prediction, mitigation, and grid resilience assessment. Its graph-structured nature makes it highly compatible with graph neural network (GNN) frameworks for node regression, edge classification, and graph classification. The naturally imbalanced failure distribution also makes it a benchmark for transfer learning and long-tail learning. The dataset is publicly available on IEEE DataPort (DOI: 10.21227/p3z3-f506), published in IEEE Data Descriptions (Volume 2, 2025).



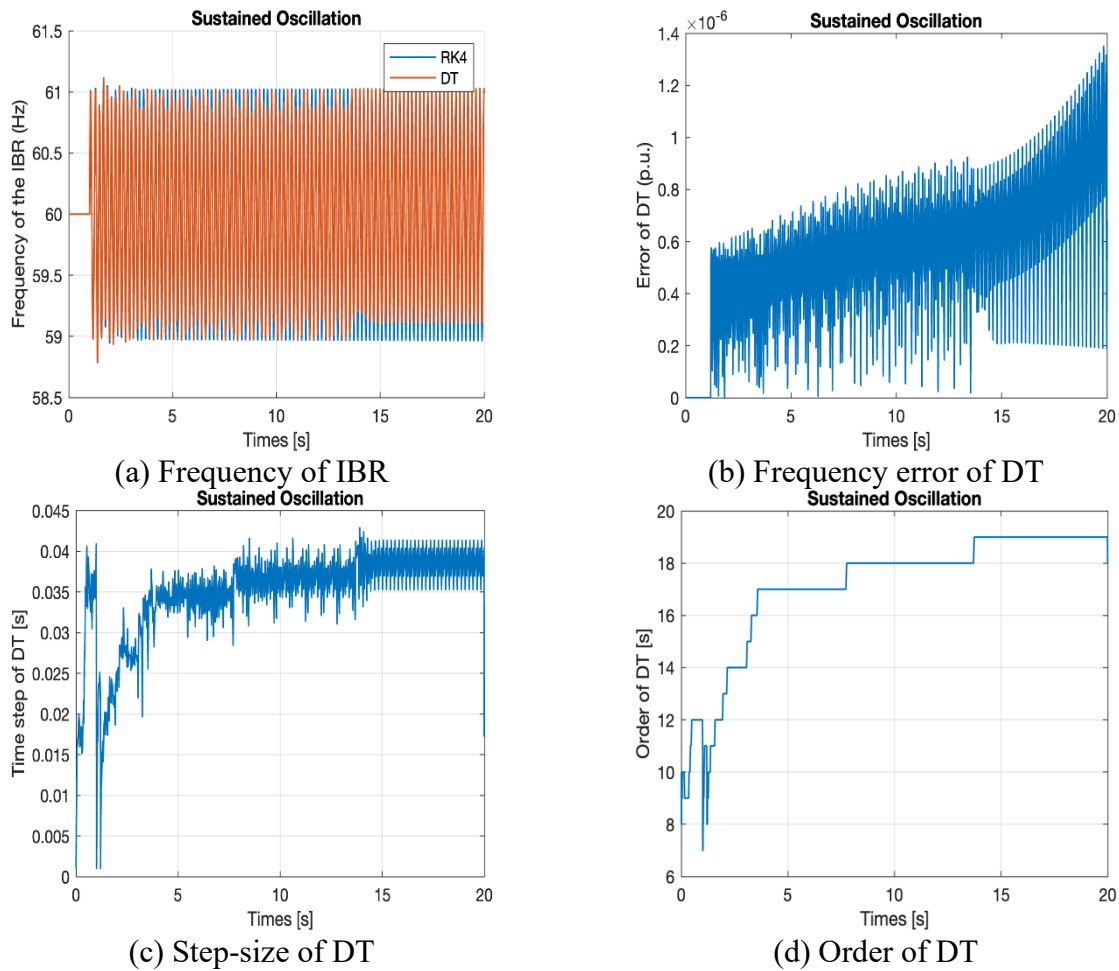


**Figure 2: Simulation results of Kundur's two-area system with IBR**

This project provides an efficient and accurate simulation framework for power systems with high penetration of inverter-based resources. The proposed method improves computational efficiency while maintaining high accuracy. Compared with traditional numerical methods, it enables larger time steps and reduces simulation time, making it suitable for stiff power system models integrating IBR models.

## 20. A Voronoi Diagram-Based Approach for AC Optimal Power Flow

<b>Project Lead:</b> Kai Sun (UTK)
<b>Graduate Students and Research faculty/associates:</b> Mohammed Khamees (UTK)
<b>Project Duration:</b> 1/2025 – 9/2025
<b>Funding Source:</b> National Science Foundation

### Summary

In this work, a new approach, shown in Fig. 1, is proposed to globally solve the AC OPF problem by exploiting the geometrical structure of the OPF search space through a computational geometry technique, the Voronoi diagram. Toward global optimization, the Voronoi diagram is applicable to characterize the search space of any dimension but requires sufficient sample points. In this paper, the sample points are efficiently added by using the continuous-projected gradient (CPG) method with enforced constraint restoration [18]. Specifically, the method constructs a fictitious nonlinear dynamical system that models the OPF solution process. The asymptotically stable equilibria of this system corresponds to local OPF solutions, whereas the other OPF critical stationary points, such as maxima and saddle points, with the OPF formulated as a minimization problem, cannot be asymptotically stable. To achieve global optimality, the Voronoi diagram provides a global, geometrical characterization of the search space by partitioning it into cells and refining it iteratively with new sampling points. These points are selected based on the geometry of the feasible set, as revealed by the diagram and heuristic insights derived from the nonlinear dynamical system.

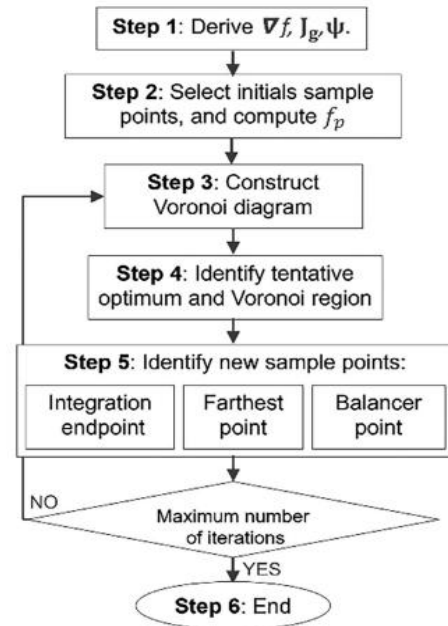


Figure 1: Flow chart

In Step 1, the proposed approach uses the CPG method with enforced constraint restoration to construct a nonlinear dynamical system described by an ordinary differential equation characterizing the flows leading to local optima. The penalized cost function constructed in Step 2 comprises the original cost function augmented by a penalty term proportional to the magnitude of constraint violations, which becomes zero when no violations are present. In Step 3 construct the Voronoi diagram is a computational geometry approach applicable to spaces of any dimension, an example is shown in Fig. 2. The candidate region, in Step 4, is defined as the Voronoi region containing the tentative optimal solution, identified as the sample point with the minimum cost function value. In the proposed approach, the CPG method with enforced constraint restoration is employed to upgrade the tentative optimum as illustrated in Fig. 3. In Step 5, enhancing the tentative optimum and improving the global approximation fidelity are two primary objectives that can be served by adding new sample points.

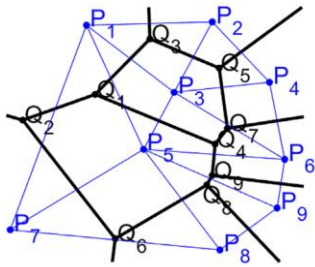


Figure 2: Voronoi Diagram

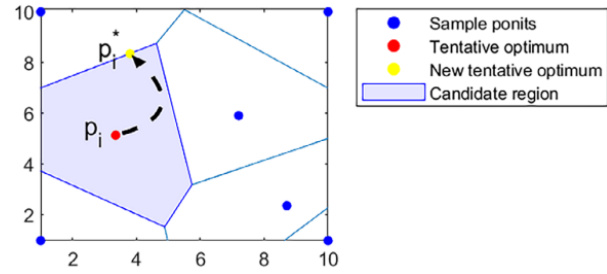


Figure 3: Candidate Region and Tentative Optimum

### Case Studies

IEEE 9-Bus System: The feasible set is five dimensions: the real output power of two generators, denoted as  $PG2$  and  $PG3$ , along with the voltage magnitudes  $V1$ ,  $V2$  and  $V3$ .

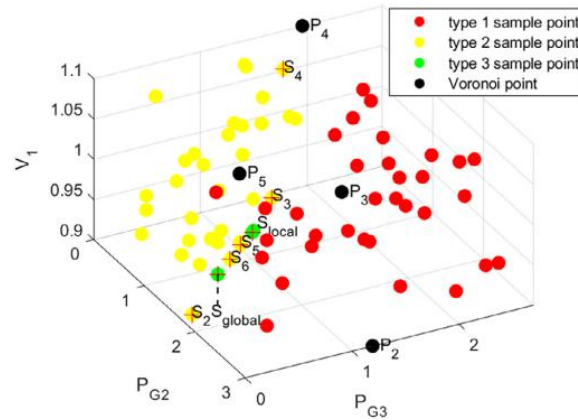


Figure 4: Case9mod: global OPF is achieved at Iteration 6

Table 1 provides a consolidated comparison of the objective value, computation time and optimality gap. As shown in the table, the proposed method achieves an optimality gap below 0.001% in all cases, whereas IPOPT failed to find the global optimum for the ‘WB5mod’ case starting from a flat initialization. In terms of runtime, the proposed method can be slower, especially for larger systems due to the time required to construct and compute Voronoi diagrams.

Table 1: Comparison between Voronoi-OPF and IPOPT

	Voronoi-OPF			IPOPT		
	Cost (\$/hr)	Time (sec)	Optimality gap (%)	Cost (\$/hr)	Time (sec)	Optimality gap (%)
<b>WB5mod</b>	139873	0.01125	< 0.001	161921	0.0209	15.76
<b>Case9mod</b>	3087.8	0.0919	< 0.001	3087.8	0.0780	< 0.001
<b>Case39mod2</b>	941.7	0.3325	< 0.001	941.7	0.1024	< 0.001
<b>Case118mod</b>	129625	10.9387	< 0.001	129625	0.1301	< 0.001

# **Power Electronics**

## 21. Assessing Grid Reliability Limits for Urban Air Mobility Integration

<b>Project Lead:</b> Kai Sun (UTK)
<b>Graduate Students and Research faculty/associates:</b> Qin Huang (UTK), Peigong Wang (UTK)
<b>Project Duration:</b> 10/2025 – 10/2026
<b>Funding Source:</b> NASA

### Summary

Urban Air Mobility (UAM) integration poses an unprecedented stress on distribution grids. High-power charging demands from UAM aircraft can lead to critical voltage drops and thermal overloads. The primary objective of this project is to develop a reliability-driven assessment framework that quantifies both individual bus and system-wide UAM load limits while identifying topology-driven "redlines" that operators must foresee.

The proposed framework, illustrated in Fig. 1, employs a two-stage exhaustive search algorithm and a vulnerability assessment module. In the first stage, the algorithm incrementally increases UAM load ( $\Delta P_i$ ) at candidate buses until safety constraints are breached. In the second stage, by exploring the defined search space, the algorithm identifies the optimal load configuration that maximizes the total UAM integration across the entire distribution system. Then, A voltage sensitivity matrix  $S_{V,PL}$  is computed to identify the "weakest" nodes. By deriving a metric  $\gamma^k$  (the sum of absolute sensitivity of Bus  $k$ ), the bus with the highest value is identified as the most vulnerable node in the topology.

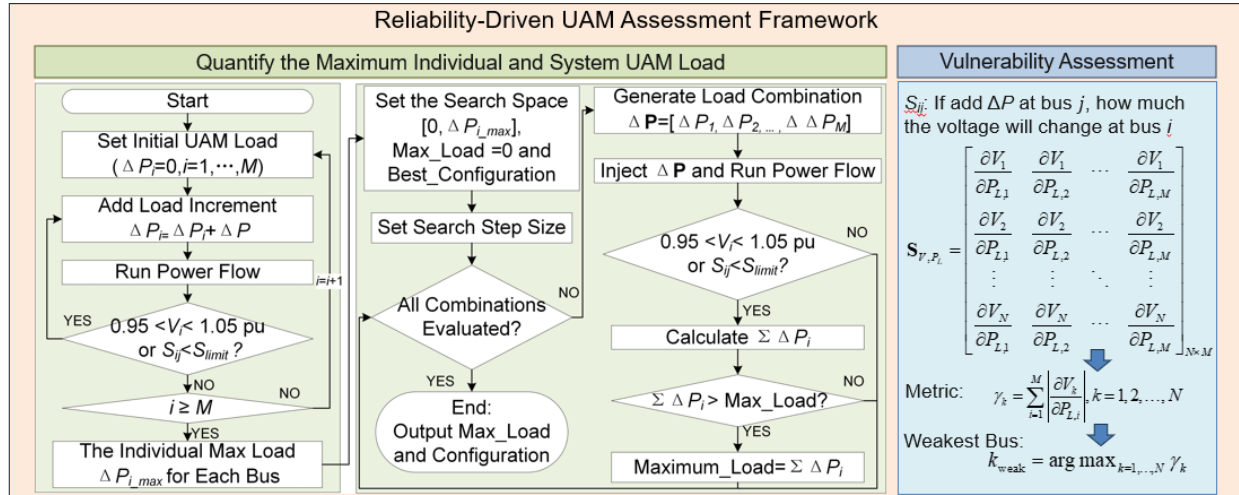


Fig.1. The framework of grid reliability assessment

For the case study, we utilized an upgraded IEEE 34-bus system, as shown in Fig. 2, scaled to a 200 MW urban load center to model dense UAM demand. This distribution testbed is coupled to a regional transmission network, which can capture the cross-layer impacts of scaling UAM loads at the transmission-distribution (T&D) interface.

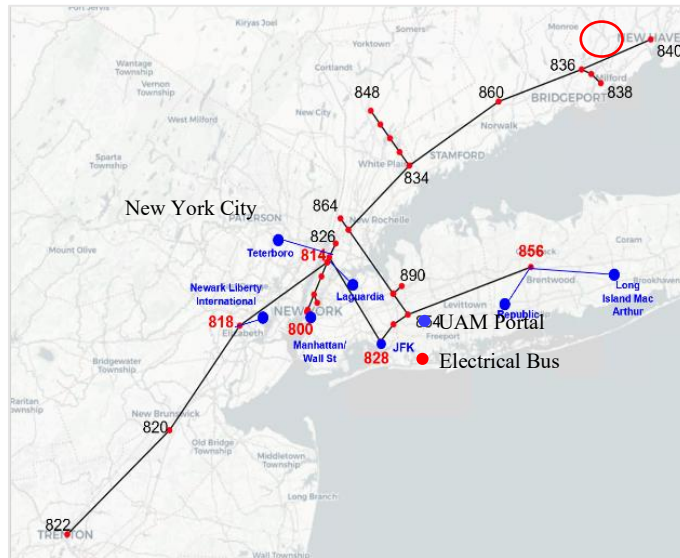


Fig.2. UAM testbed mapped onto the New York City region.

The assessment identified the specific "Individual Max Load" for each candidate bus. Based on these individual limits, the "System-wide Maximum UAM Load" and its corresponding optimal configuration were determined, reaching a total capacity of 84.5 MW (Table 1). Furthermore, the sensitivity analysis identified Bus 840 as the weakest node in the grid, exhibiting the highest sensitivity to load fluctuations ( $\gamma^{840} = 1.809 \times 10^{-3}$ ).

Table 1. Search Bounds and System-wide Maximum UAM Load

UAM Bus	Search Space	Step Size (MW)	System Optimal Configuration (MW)
814	[0, 11.1375]	0.1	11
828	[0, 6.3]	0.1	6.2
856	[0, 15.4]	0.1	6.0
800	[0, 56.25]	0.5	54.0
818	[0, 5.85]	0.1	5.8
<b>Total Capacity</b>	/	/	<b>84.5</b>

The proposed reliability assessment framework quantifies the operational boundaries for large-scale UAM integration and identifies Bus 840 as the most vulnerable node. These findings provide critical decision support for utilities to develop precise grid reinforcement plans and capacity management strategies when addressing future high-penetration transportation loads.

## 22. Integrated Three-level GaN Inverter and PMSynRM Motor for Electric Passenger Vehicles and Medium/heavy duty Trucks (GaNIn\_PMSynRM)

**Project Lead:** Kevin Bai (UTK), Daniel Costinett (UTK), Leon M. Tolbert (UTK)

**Graduate Students and Research faculty/associates:** Niu Jia (UTK), Yicheng Zhang (UTK), Xianchao Liu(UTK), Anwasha Mukhopadhyay(UTK), Noah Wilding(UTK)

**Project Duration:** 6/2024 – 8/2027

**Funding Source:** DOE-VTO

### Summary

The objective of this project is to develop and integrate an 800V/200kW Gallium Nitride (GaN\_- based three-level high-power-density inverter and Permanent Magnet assisted synchronous Reluctance Motor (PMSynRM). The inverter will meet all performance targets of >99% efficiency at rated power, >110kW/L volumetric density, \$2.2/kW cost. The novel PMSynRM using alternative magnet material and liquid cooling will achieve more than 55kW/l at <\$3.3/kW. Together, this innovative, integrated electric traction motor and drive will meet the aggressive, >33 kW/L volume density and <\$6/kW cost system targets.

The project will have three budget periods lasting 39 months. The University of Tennessee, Knoxville (UTK) is the project lead. In addition to the project management, UTK will develop the inverter packaging, control, and test. Four subrecipients include ABB Inc (motor design, control, and test), University of Michigan-Dearborn (UMD, topology selection and simulation), Rensselaer Polytechnic Institute (RPI, gate driver development) and Oak Ridge National Laboratory (ORNL, thermal solutions and dynamometer test). Lucid USA will provide contractual services, focusing on system specs, design guidance, reliability analysis and technology-to-market (T2M) plan.

In the present budget period, UTK packaged GaN based power module and processed the double pulse test (DPT). The test results indicated <100V voltage spike to secure the GaN reliability. In BP2, the team will start to package the whole inverter.

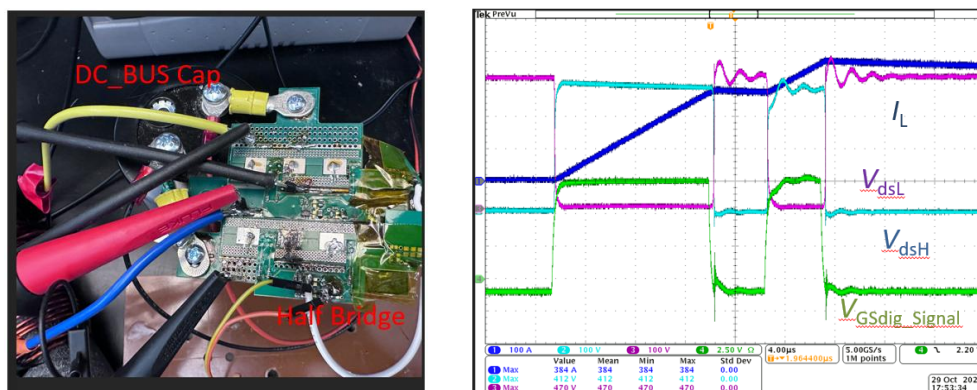


**Fig.1. DPT results of the packaged GaN power module: (left) test bench and (right) switching waveform @400 V/385 A.**

## 23. Characterization of DFPAK and Evaluation of DFPAK in an Inverter Application

**Project Lead:** Kevin Bai (UTK)

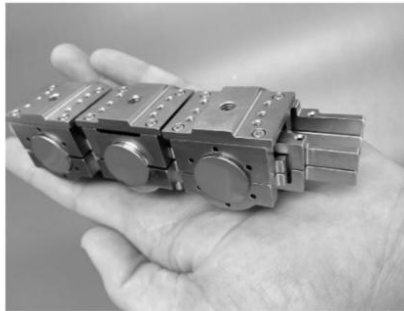
**Graduate Students and Research faculty/associates:** Xin Xia, Yicheng Zhang, Saleh Khan (UTK)

**Project Duration:** 12/2025 – 6/2026

**Funding Source:** Diamond Foundry

### Summary

This proposal will involve power electronics team from The University of Tennessee, Knoxville (UTK) to characterize DFPAK devices packaged by Diamond Foundry (DF) and build and test the inverter based on such device. Both electrical and thermal tests will be carried out by the UTK team to understand the benefits of using diamonds as thermal interface material, e.g., low thermal impedance thereby smaller footprint, as well as its system-level in electric vehicle (EV) drive inverters. At the end of the project, UTK team will carry out high voltage and high current test using an RL load. Voltage and current harmonics, efficiency/loss, as well as temperature profile of the DFPAK over the testing range will be recorded. A 800V/200kW EV inverter will be the final delivery.



### DF Perseus Power Inverter

POWER (KW): 250  
SIC CHIPS: 18  
VOLUME (L): 0.46  
DENSITY (KW/L): 500

**Fig.2. Diamond Foundry Inverter (<https://www.df.com/power-electronics> )**

## 24. Characterization of HV bi-directional GaN devices and development of 22kW bidirectional GaN devices based three-phase single-stage wireless battery charger for electric vehicles

<b>Project Lead:</b> Kevin Bai
<b>Graduate Students and Research faculty/associates:</b> Xin Xia, Yicheng Zhang, Saleh Khan (UTK)
<b>Project Duration:</b> 12/2025 – 12/2026
<b>Funding Source:</b> BMW

### Summary

This project will involve graduate research assistant students of power electronics from The University of Tennessee, Knoxville to

1. Characterize high voltage bi-directional GaN devices based on test specification from BMW. The characterization will be carried out to evaluate different bi-directional GaN switches available. The auxiliary systems such as gate driver or sensing and protection circuitry needed for the characterization will either be purchased or designed and fabricated.
2. Design and develop three-phase single-stage wireless power transfer (WPT) system for BMW North America, using 650V bidirectional GaN devices on the grid side, 1200V SiC MOSFETs on the receiver side to accommodate an 800V battery. Based on the specifications provided by BMW, UTK team will study and simulate the best topology for a three-phase single-stage 22kW EV WPT, incorporate with bidirectional GaN and poly-phase WPT transmitters and receivers, lay out the circuit including magnetics, power electronics components and heatsink, etc, prototype the whole WPT and carry out the full voltage and power test. The project will evaluate the merits of bidirectional GaN enabled single stage wireless charging wallbox e.g., lower cost and smaller footprint thereby higher power density.

## 25. A High-efficiency and High-power-density 48/12V DC/DC Converter for Electric Vehicles

**Project Lead:** Kevin Bai (UTK), Daniel Costinett (UTK)

**Graduate Students and Research faculty/associates:** Saleh Khan (UTK), Yicheng Zhang (UTK)

**Project Duration:** 11/2024 – 12/2025

**Funding Source:** Hella/Fovia

### Summary

The final deliverable of this project is a 48V/12V DCDC converter used for electric vehicles (EVs), with the input range of 36V~60V and the output voltage of 12V. The UTK team will offer the modular design of 1kW, 2kW and 4kW. It is desired to use wide-bandgap devices particularly GaN to reach high efficiency (>97%) and high-power density (>13kW/L). The goal is to reach high compactness and low cost.

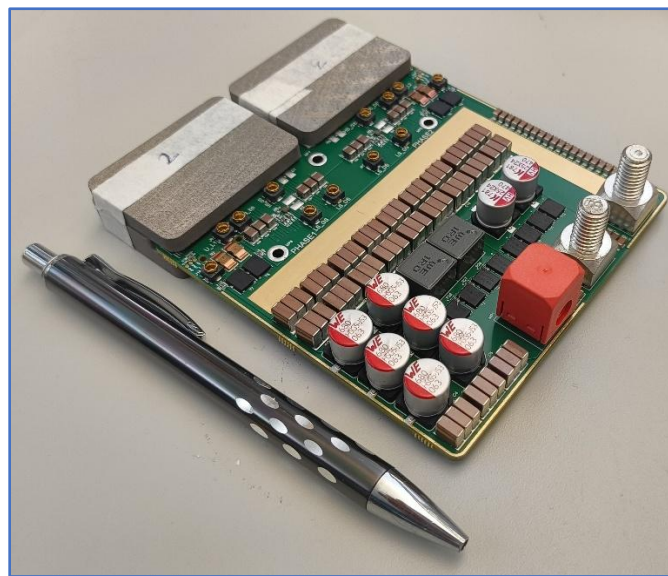


**Fig.3. UTK developed 4kW dc-dc converter**

## 26. A GaN based DC/DC Converter Using Planar Technology for Electric Vehicles

**Project Lead:** Kevin Bai (UTK), Daniel Costinett (UTK)

**Graduate Students and Research faculty/associates:** Saleh Khan (UTK), Yicheng Zhang (UTK)

**Project Duration:** 11/2024 – 12/2025

**Funding Source:** Hella/Fovia

### Summary

The final deliverable of this project is a DCDC converter used for electric vehicles (EVs), with the input range of 180V~940V and the output voltage of 6V~16V. The rated power is 4kW. It is desired to use wide-bandgap devices to reach high efficiency (>95%) and high-power density (>5kW/L), such as 1200V GaN with two level design, or 650V GaN with a three-level topology.

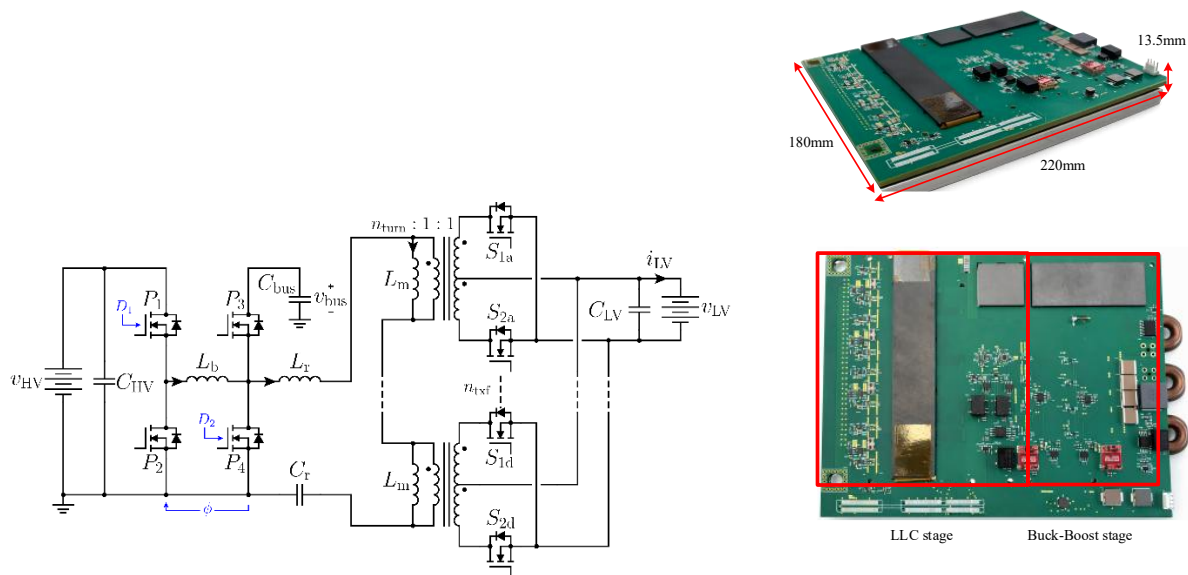


**Fig.4. UTK developed dc-dc converter: topology (left) and prototype (right)**

## 27. Integrated Zero-Emission Aviation using a Robust Hybrid Architecture

**Project Lead:** JiangBiao He (UTK)

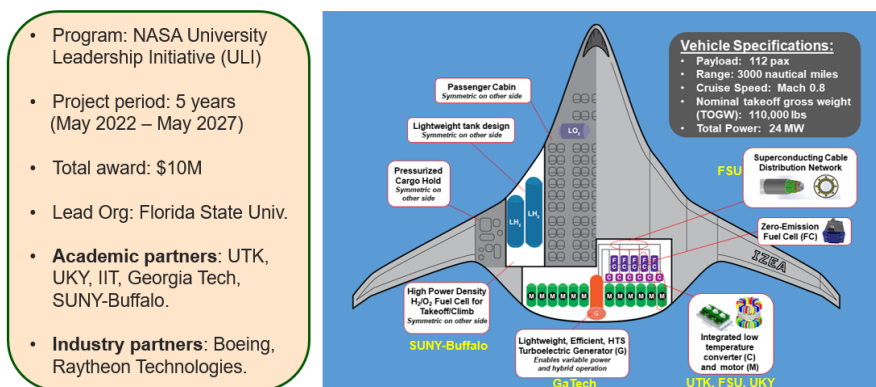
**Graduate Students and Research faculty/associates:** Farzad Y. Notash (UTK)

**Project Duration:** 05/2022 – 05/2027

**Funding Source:** NASA (Lead: Florida State University)

### Summary

The proposed project is an academic-industry collaboration focused on achieving zero emissions from longer-range (>3000 nautical miles) aircraft transporting at least 100 passengers. Avoidance of CO<sub>2</sub> emission motivates novel hybrid hydrogen-electric propulsion architectures. Our approach considers hybrid electric power generation via a combination of turboelectric generators and fuel cells (FC) using liquid hydrogen. Avoidance of NO<sub>x</sub> emission, efficiency augmentation, and high-power mission segments drive consideration of liquid oxygen (LO<sub>x</sub>) during takeoff and climb. The cryogenics facilitate use of superconductors to increase power density of the distribution system, generators, and motors, and the presence of multiple temperature zones from 20 to 400 K offers opportunities to decrease the impact of thermal management systems on efficiency and weight. Experts in electric power, energy storage/conversion, propulsion, cryogenics, superconductivity, thermal management, motors, power electronics and distribution, and aircraft systems with an extensive collaborative history and unmatched capabilities and facilities will conduct modeling, design trade studies and multi-disciplinary design optimization, combined with subsystem demonstrations of key components for validation and implementation.



### Key Objective:

The UTK team's project objective is to support the hybrid-electric aircraft propulsion inverter and motor development, in addition to leading the tasks of motor control and online health monitoring of the propulsion drive systems.

## 28. Multi-Input Integrated Smart Charger-Inverter System for Electric Vehicles

**Project Lead:** JiangBiao He (UTK)

**Graduate Students and Research faculty/associates:** Abdel Habib (UTK)

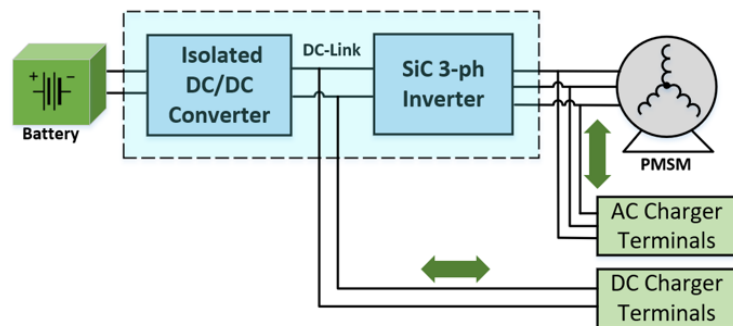
**Project Duration:** 11/2024 – 11/2027

**Funding Source:** Department of Energy (Lead: Western Michigan University)

### Summary

This project is to develop integrated charger-inverter (ICI) technologies that enable existing electric vehicle (EV) inverters to serve as a bi-directional charger, while optimizing the overall system for high efficiency, high power density, and low cost, eliminating the need for on-board or off-board chargers. The elimination of a separate charger dramatically reduces overall system cost, mass, and volume while enabling the vehicles to seamlessly integrate with vehicle-to-grid (V2G) and charging while driving technologies. Advanced magnetics and dual active bridge based galvanic isolation enable real-world high-power energy transfer to the vehicle. The hardware developed will be integrated into a vehicle and validated across a range of charging, driving, and regenerative braking profiles. The project is only possible through DOE funding and it facilitates outcomes and impacts aligned with the DOE VTO/EERE mission.

- Project period: 3 years (2024 – 2027)
- Total project award: \$3.179M
- Lead Org: Western Michigan Univ.
- **Academic partners & national lab:** UTK, UKY, ORNL
- **Industry partners:** John Deere Corporation, and BorgWarner Inc.



### **Key Objective:**

The UTK team's project objective is to develop and demonstrate a 150-kW integrated charger-inverter system that contains multiple input interface for both AC and DC fast charging, compatible for both 400V and 800V EV systems, at high efficiency (>98%) and high power density (>10kW/L).

## 29. Electric Machines with Adaptive Surge Impedance

**Project Lead:** JiangBiao He (UTK)

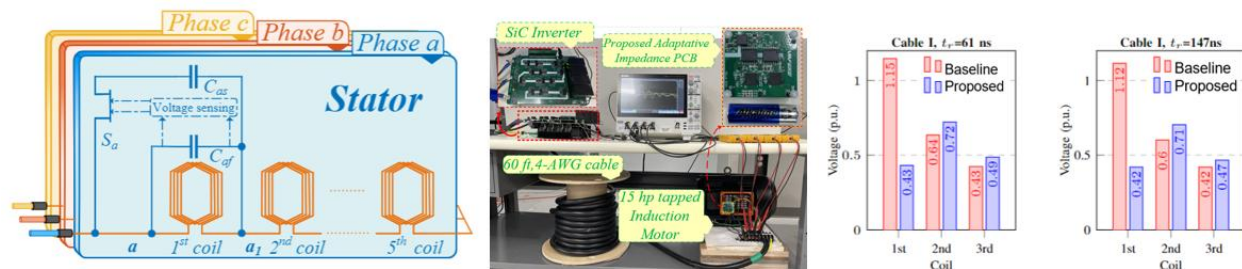
**Graduate Students and Research faculty/associates:** Mohamed Farag (UTK)

**Project Duration:** 04/2022 – 07/2026

**Funding Source:** Office of Naval Research (ONR)

### Summary

Recent advancements in power electronics have enabled more-electric propulsion systems, realizing higher efficiency, lower acoustic noise, lower emissions, and less operating costs. Furthermore, power electronic devices with higher voltage levels such as medium-voltage DC (MVDC) and faster semiconductor switches are desired to design electric propulsion systems to achieve higher efficiency and power density. The combination of these desired technologies results in undesired technical challenges for propulsion motor designers. The high voltage rate creates traveling waves in the cables between the drive and motor, and thus, generates high-frequency voltage ringing across the stator windings with high-voltage spikes. This voltage stress has adverse effects on the motor, including motor insulation stress and harmful bearing currents. Though this is a known phenomenon, the trend toward using wide bandgap (WBG) switches, such as Silicon Carbide (SiC) and Gallium Nitride (GaN) power transistors, in propulsion systems requires novel solutions to mitigate the high-frequency high-voltage stress that degrades the motor lifetime. The voltage stress on motor insulation can conduct to incipient faults, a cascaded propulsion system's failure, and extra expenses associated with unexpected maintenance. We propose an adaptive surge impedance solution to enhance motor performance in WBG-based motor-drive systems, which adaptively matches surge impedance of the cables and the motor.



### Key Objective:

This project aims to develop an adaptive surge impedance technology for propulsion AC motors that can mitigate any reflected surge voltages, without compromising the power density and efficiency of the motor-drive systems in safety-critical propulsion applications such as electric ships. Specifically, the motor coil surge impedance can be automatically adjusted in the adaptive surge impedance technology by implementing a parallel variable impedance branch based on WBG switches. The merit of the proposed technology is eliminating the need for any bulky and lossy passive filters.

### 30. Advanced Immersion Cooled Power Electronic Converters

**Project Lead:** JiangBiao He (UTK)

**Graduate Students and Research faculty/associates:** Yiju Wang (UTK), Reza Ilka (UTK)

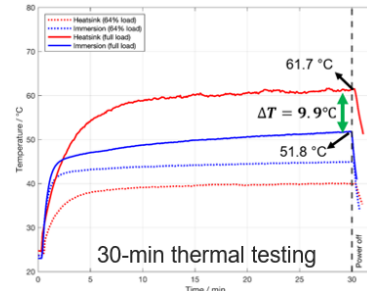
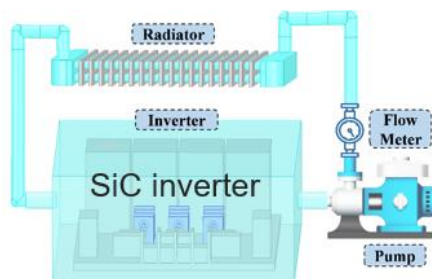
**Project Duration:** 07/2023 – 08/2026

**Funding Source:** Valvoline Global Operations

#### Summary

Power electronic converter is a critical power management unit interfacing battery energy storage and traction motor for electric propulsion systems in transportation vehicles (ground vehicles, aircraft, ships, etc.). Generally, the most important criteria to evaluate the technical performance of a power converter include: energy efficiency, reliability, cost, and power density (i.e., size and weight). The conventional air cooling or indirect liquid cooling technologies significantly constrain the further improvement of power converters' efficiency, reliability, and power density. Thus, it is indispensable to develop novel cooling technologies.

Based on the continuous support from Valvoline Global Operations, our team has investigated the thermal management capability of immersion cooled power converters, in comparison to conventional air-cooled power converters. Our multi-physics modeling, simulation, and preliminary experimental verifications show that the immersion cooled power converters have significant advantages over the traditional cooling methods, such as homogenous cooling for all the power devices, elimination of thermal runaway risks, and dramatically improved dielectric insulation capability.



#### **Key Objective:**

- (1) Conduct comparative experiments between the immersion cooling and the conventional cold plate based indirect liquid cooling. Under the same operating conditions, we plan to characterize the specific benefits of immersion cooled power electronics versus its counterpart with cold plate based indirect liquid cooling.
- (2) Considering that immersion cooling is much more homogenous on thermal management of power electronics, which is expected to mitigate the aging/fatigue of soldering joints on the power circuit boards or semiconductor modules.
- (3) Dielectric insulation testing to demonstrate the merits of immersion cooled SiC converters.

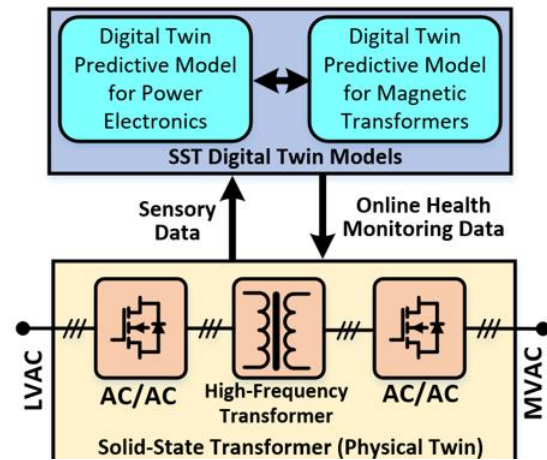
### 31. Digital Twin Predictive Health Monitoring of Solid-State Transformers

<b>Project Lead:</b> JiangBiao He (UTK)
<b>Graduate Students and Research faculty/associates:</b> Xin Gao (UTK)
<b>Project Duration:</b> 09/2023 – 09/2026
<b>Funding Source:</b> National Science Foundation (NSF)

#### Summary

Solid state transformer (SST), a new type of smart power electronic transformer which is much more compact than the conventional electromagnetic transformer, has been deemed as a revolutionary technology for future-generation power systems. However, one major technical barrier that constrains the further development of SST is the low reliability compared to the conventional electromagnetic transformers, due to the large number of semiconductor devices utilized. Currently, the reliability of SST has received little attention. To address this challenge, this project will develop a comprehensive systematic framework of online health monitoring for resonant SSTs, in order to significantly improve the reliability to electric failures.

The proposed health monitoring framework will include online prognosis and diagnosis of potential electrical faults that could occur to SST, targeting at common semiconductor switching faults and health degradation in the high-frequency magnetic transformers. Specifically, a portfolio of critical SST parameters will be monitored through a smart gate driver that will be integrated with the power electronic building blocks, so any degradation in the semiconductor modules can be predicted and diagnosed during the fault incipient stage. Active power cycling lifetime extension method for semiconductor modules through improved control strategies will also be developed and implemented, if the estimated lifetime of power converters degrades below a pre-determined threshold target. For the high-frequency transformer within the SST, advanced health monitoring digital twin model will be established, so major electrical aging in the transformer windings and magnetic cores can be predicted online.



#### Key Objective:

- Develop digital twin based predictive health monitoring models for SST power electronics.
- Develop digital twin based predictive health monitoring models for the winding insulation degradation of the high-frequency transformers in SSTs.
- Experimental verifications of the digital twin models.

## 32. Multiport Quad-Active-Bridge Converters for PV-Battery-EV-Grid Systems

**Project Lead:** JiangBiao He (UTK)

**Graduate Students and Research faculty/associates:** Aaqib Sheikh (UTK), Jim Camp (UTK)

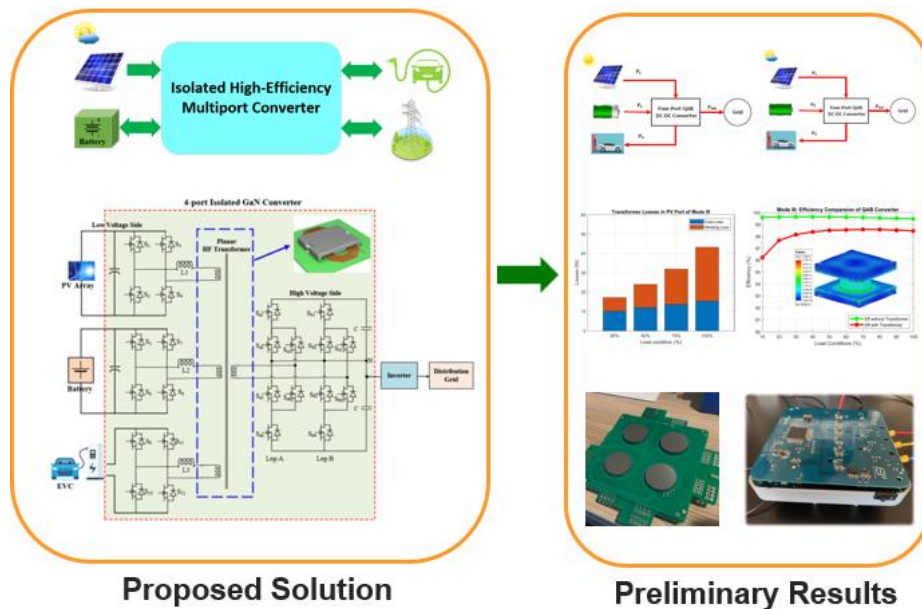
**Project Duration:** 11/2024 – 09/2026

**Funding Source:** Department of Energy (DOE)

### Summary

The net-zero energy buildings (NZEBs) market is expanding rapidly and is projected to significantly increase in value, highlighting the critical role of innovative energy solutions in achieving sustainable development and reducing global energy disparities.

The proposed Quad-Active-Bridge (QAB) DC-DC converter and high-frequency planar transformer technologies are cost-effective and scalable solutions to form a multiport converter to meet the market challenges for isolated high-efficiency and low-cost power converters. They offer an efficient way to interconnect distributed solar power, energy storage, and EV charging stations, providing a modular, scalable, and high-efficiency energy management solution. These technologies enhance energy distribution and utilization and align with the growing market demands, particularly in net-zero energy buildings.



### **Key Objective:**

- GaN based 15-kW QAB converter hardware prototyping
- Multiport high-frequency planar transformer design and optimization
- QAB converter testing at various operation modes to meet the interconnection standards of distribution grid

### 33. A Generalized Physics-Based Circuit Model for Predicting Nonlinear Properties of Magnetic Materials.

<b>Project Leads:</b> Leon M. Tolbert (UTK), Gong Gu (UTK), Daniel Costinett (UTK)
<b>Graduate Students and Research Faculty/Associates:</b> Sadia Binte Sohid (UTK), Noah Wilding (UTK), Christian Harmon (UTK)
<b>Project Duration:</b> 8/2022 – 07/2026
<b>Funding Source:</b> Office of Naval Research (ONR)

#### Summary

The nonlinear and frequency-dependent behavior of magnetic materials continues to limit the accuracy of conventional magnetic models, especially in high-frequency power electronics where core loss and permeability vary with excitation conditions. To overcome the limitations of conventional models, the

spherical form of the LLG equation (sLLG):  $\begin{bmatrix} \frac{d\theta}{dt} \\ \frac{d\varphi}{dt} \end{bmatrix} = \mu_0 \frac{\gamma}{(1+\alpha^2)} \begin{pmatrix} \alpha & 1 \\ -\frac{1}{\sin\theta} & \frac{\alpha}{\sin\theta} \end{pmatrix} \begin{bmatrix} H_{eff}^\theta \\ H_{eff}^\varphi \end{bmatrix}$  is used to

model magnetization dynamics. An important advantage of the sLLG is that it inherently preserves the constant magnetization magnitude, avoiding the additional numerical constraints required in the Cartesian LLG model. The spherical LLG approach reproduces the same overall hysteresis behavior as the full LLG formulation while greatly reducing simulation time.

Effects due to magnetic anisotropy as well as domain coupling are incorporated into the dynamics governing the system. Domain magnetic moments change over time when subjected to an external magnetic field, as illustrated in Fig. 2. Magnetic anisotropy is illustrated in Fig. 3 and shows how anisotropic materials prefer to align their magnetic moments with the easy axis. To extend the model beyond a single-domain approximation, the material is represented as a coupled two domain system in which neighboring domains interact through domain-wall energy, as illustrated in Fig. 4.

To reduce the total computation power and time required of this model, the precessional motion term can be omitted as it has a negligible effect on energy loss through damping. The resulting simplified spherical LLG (ssLLG)  $\frac{d\theta}{dt} = \mu_0 \frac{\gamma}{(1+\alpha^2)} (\alpha H_{eff}^\theta + H_{eff}^\varphi)$  equation preserves dominant system dynamics while requiring far less simulation time than the cartesian LLG approach as illustrated in Fig. 5.

The coupled model accounting for both anisotropy and domain wall motion was simulated, and results comparing the sLLG and ssLLG are shown in Fig. 6. The ssLLG model shows good alignment with the full sLLG model while requiring minimal runtime.

Future project work includes incorporation of multiple coupled domains as well as temperature dependence of material properties such as anisotropy constant, magnetic saturation, and exchange stiffness. Collaboration with magnetics material developers at the University of Pittsburgh, Northeastern University and Dartmouth University will aid in ensuring the model can predict the behavior of new magnetic materials.

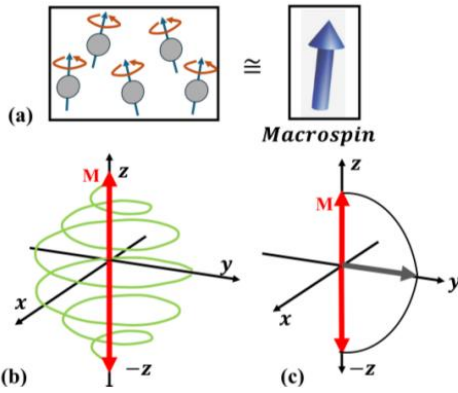


Fig. 1. (a) Equivalent macrospin model representing the collective magnetization ( $M$ ) of the system under an effective magnetic field ( $H_{eff}$ ) (b) Dynamic motion of a dipole moment governed by the LLG equation. (c) Two equilibrium magnetization states predicted by energy minimization theory.)

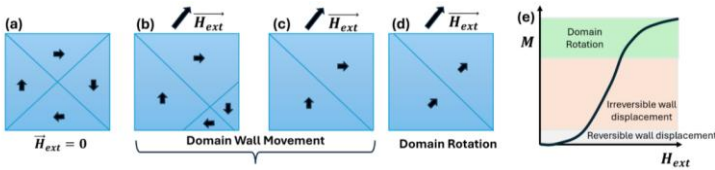


Fig. 2. Illustration of the progression of magnetization in a crystal under an applied magnetic field. Starting from the demagnetized state in (a), where domains with different magnetization orientations are present, the application of an external field initiates domain wall motion, as shown in (b) and (c). This wall movement leads to the growth of domains aligned with the field direction. As the field strength increases further, the process transitions from domain wall motion to rotation of magnetization, as shown in (d). The corresponding magnetization curve in (e) highlights the distinct regions associated with reversible wall motion, irreversible domain wall displacement, and domain rotation

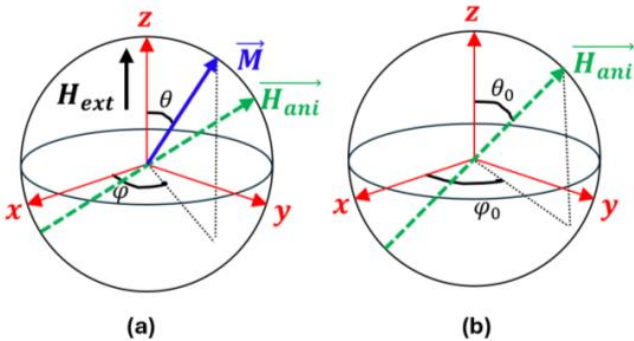


Fig. 3. Illustration of the magnetization vector  $M$  and anisotropy field  $H_{ani}$  in spherical coordinates, defined by angular components  $(\theta, \varphi)$ , and  $(\theta_0, \varphi_0)$ , respectively.

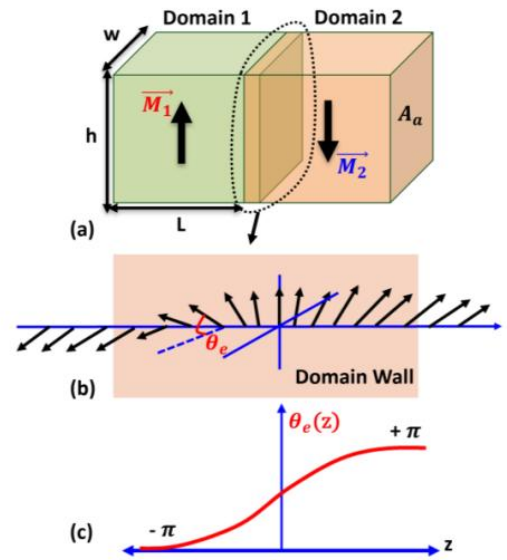


Fig. 4. Two-domain model: (top) domains 1 and 2 magnetized  $180^\circ$  apart; (middle) spins rotate through angle  $\theta_e$  in the wall, balancing exchange and anisotropy torques; (bottom) continuous  $\theta_e(z)$  profile across the domain wall.

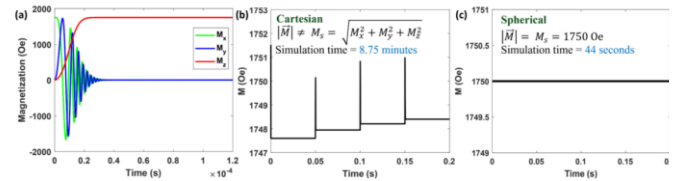


Fig. 5. Comparison of LLG simulations in cartesian and spherical coordinates. (a) Magnetization dynamics computed using both cartesian and spherical coordinates. (b) The cartesian model shows deviation from the constant magnitude condition ( $|M| = M_s$ ) and requires a longer runtime (8.75 min). (c) The spherical model maintains constant  $|M| = M_s$  with faster runtime (44 s).

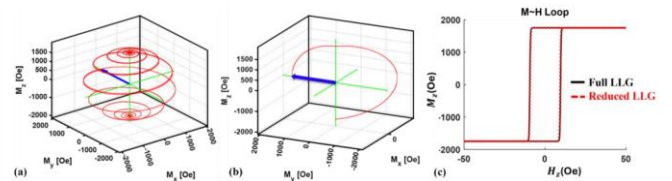


Fig. 6. Here,  $M_s = 1750$  Oe,  $\alpha = 0.1$ ,  $f = 10$  kHz [11]. Dynamic motion using (a) the full LLG equation and (b) the reduced LLG equation. The aligned M-H loops for both cases confirm consistency in magnetization behavior

### 34. Co-located SMRs, hyperscale data centers, and energy storage for increased system resiliency

<b>Project Lead:</b> Leon M. Tolbert (UTK)
<b>Graduate Students and Research Faculty/Associates:</b> Mariana Espinola (UTK), Mateus Silva (UTK), Hari Naicker (Nuclear Engineering, UTK), Justin Zondor (NE, UTK), Carlos G. Zevallos, Shiyuan Fan (UTK), Jamie Coble (Nuclear Engineering, UTK)
<b>Project Duration:</b> July 2025 – June 2026
<b>Funding Source:</b> UT-ORII

#### Summary

This project proposes a grid-connected microgrid architecture centered on a Small Modular Reactor (SMR) as the primary power source for a hyperscale data center. The proposed system considers the integration of thermal energy storage (TES), a Battery Energy Storage System (BESS), and a coordinating Energy Management System (EMS) to support the facility’s load while enabling potential participation in electricity markets through ancillary service provision.

The data center load is being represented using simplified demand scenarios intended to approximate the scale and variability expected in next-generation hyperscale deployments. These scenarios are designed to capture characteristics associated with both inference and training workloads, which can exhibit large magnitude and rapid temporal variation.

In the proposed operating strategy, the SMR is assumed to operate near full capacity to maintain a high capacity factor, while the BESS is used to compensate for short-term mismatches between quasi-steady nuclear generation and fluctuating IT load. The electrical storage subsystem is currently represented using a containerized lithium-ion BESS architecture with an initial target rating of approximately 120 MW / 480 MWh for transient smoothing and contingency support; however, storage sizing remains under evaluation as part of the ongoing system design process. Waste heat recovered from the SMR is also considered as a potential resource for thermal energy storage and cogeneration applications that may improve site-level energy utilization and Power Usage Effectiveness (PUE).

A hierarchical EMS framework is being developed to coordinate dispatch across SMR, BESS, and TES subsystems. At the supervisory level, the controller is intended to maintain reliable power delivery to the data center while respecting SMR ramp-rate constraints and managing storage utilization. Local control layers regulate battery power response, TES scheduling strategies, and grid import/export behavior under representative operating conditions.

Current work focuses on system architecture definition, component sizing assumptions, and the development of coordinated control strategies under representative load scenarios and grid operating conditions. The modeling framework is intended to support future evaluation of techno-economic performance, regulatory and interconnection considerations, and scalability to multi-module SMR configurations for large data center campuses.

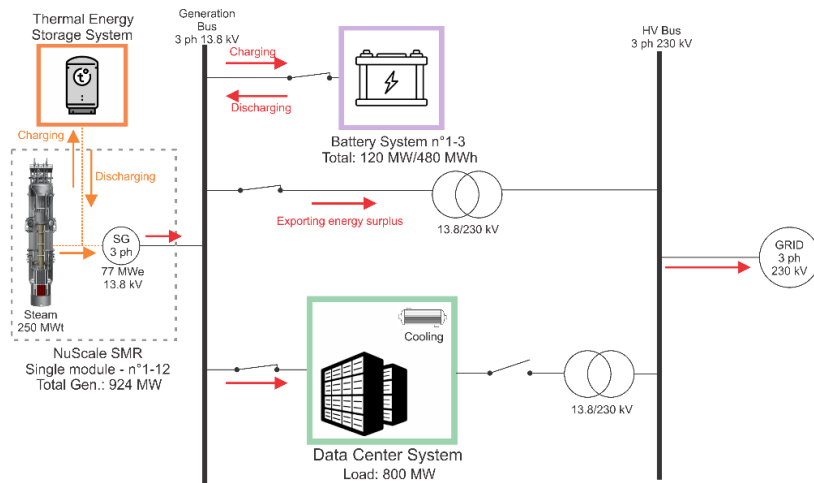


**Figure 1.** Integrated SMR–TES–BESS architecture supplying a hyperscale data center with grid interconnection capability.

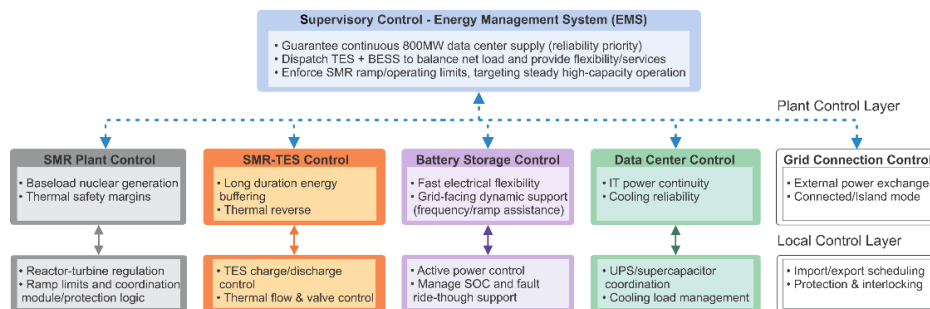


**Figure 2.** Hierarchical supervisory and local EMS control structure coordinating SMR operation, storage dispatch, and data center load support.

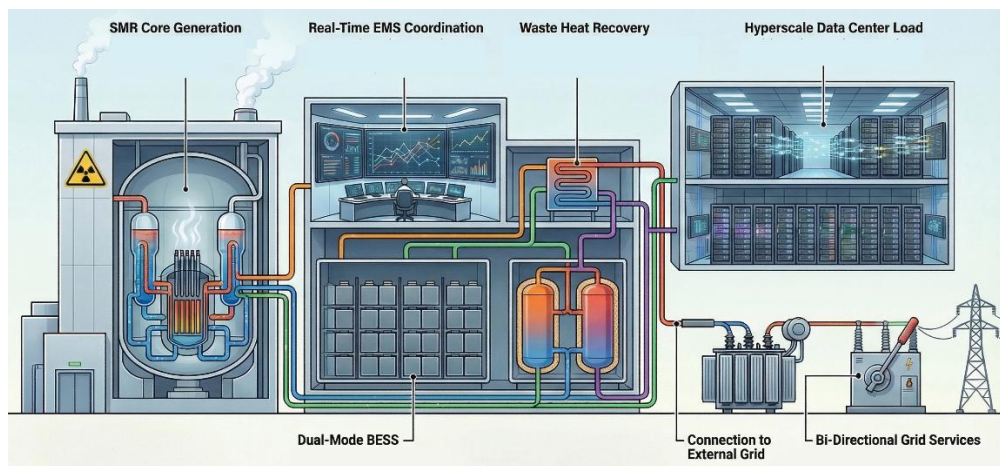


**Figure 3.** Representative operating scenarios for coordinated SMR–TES–BESS support of hyperscale data center operation.

### 35. An Ultra-Light Tightly-Integrated Modular Aviation Transportation Enabling Solid-State Circuit Breaker (ULTIMATE-SSCB)

<b>Project Lead:</b> Fred Wang (UTK), Kevin Bai (UTK), Zheyu Zhang (RPI), Ruirui Chen (UTK)
<b>Graduate Students and Research faculty/associates:</b> Jimmy Yang (UTK)
<b>Project Duration:</b> 7/2021 – 6/2025
<b>Funding Source:</b> ARPA-E

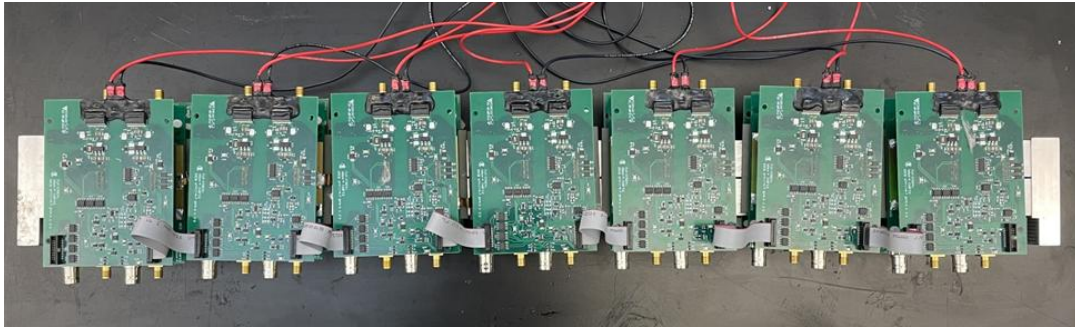
#### Summary

The project aims at developing and testing in simulated flying environment an ultra-light tightly-integrated modular aviation-transportation enabling solid-state circuit breaker (ULTIMATE-SSCB). The proposed ULTIMATE-SSCB will meet several objectives important for future electrified aircraft propulsion (EAP) systems: extremely light, efficient, fast, reliable, suitable for future medium voltage EAP system at >10 kV DC, taking advantages of cryogenic cooling enabled by liquified natural gas (LNG) or liquid hydrogen fuel of future EAP system. The developed SSCB will be highly flexible with modular structure, intelligent and easy for protection coordination and system integration, with built-in directional function, and current limit function.

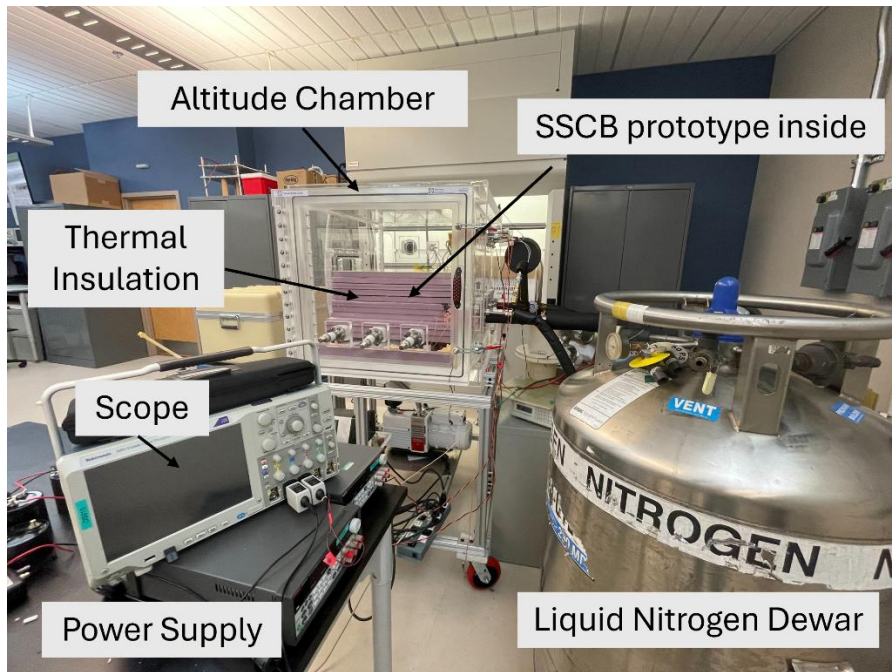
In phase I of the project, the team identified the specification and requirements of the 10 kV, 100A SSCB and completed conceptual design of the SSCB using cryogenically cooled GaN devices and key components testing. The SSCB is designed to interrupt up to 10x current during fault. Design of modularized SSCB, sensors, intelligent gate driver, control and communication strategy have been developed. A notional electrified aircraft propulsion architecture is identified and investigated with simulation to determine capability requirement of SSCB and to validate the protection and co-ordination strategy.

In phase II of the project, the team has developed a 750V, 100A SSCB module that can be used in 5 kV unipolar or a 10 kV bipolar MVDC system. A series combination of 14 such modules will meet the requirements of 10 kV, 100A SSCB for future EAP system. A liquid Nitrogen based cooling system is developed and the module is successfully tested to interrupt a fault current of 1 kA. A cryogenic packaging for the module is developed and the module is successfully achieved high efficiency (>99.96%), compact (255.22 kW/L), light(350.95 kW/kg) and highly integrated with embedded functions including gate-drive based protection and current limiting. The module is also designed for high-altitude operation and successfully tested in an emulated high-altitude test setup.

In phase III of the project, the team has constructed the 5kV, 100A SSCB prototype using 7 of 750V, 100A SSCB modules. The prototype successfully interrupted 10X fault current (1kA) and achieved >99.96% of the efficiency with cryogenic cooling. The prototype also successfully passed the insulation test in the simulated high-altitude environment with cryogenic cooling. The 5kV prototype is verified to withstand 8 kV at emulated 40,000 ft environment.



(a)



(b)

**Figure 1: (a) 5kV, 100A prototype, (b) High altitude test setup**

### 36. A UNIVERSAL (Ultrafast, Noise-Immune, Versatile, Efficient, Reliable, Scalable, and Accurate Light-controlled) Switch Module

**Project Lead:** Fred Wang (UTK), Kevin Bai (UTK), Ruirui Chen (UTK), Kaushik Rajashekara (UH), Zheyu Zhang (RPI), Hai Xiao (Clemson), Fei Lu (Lehigh), Steve Schmalz (Eaton), Mark Mevey (Dominion), Shengyi Liu (Boeing)

**Graduate Students and Research faculty/associates:** Yang Xu (UTK), Xingyue Tian (UTK), Samuel Klein (UTK), Shahabuddin Khan (RPI), Yongji Wu (Clemson), Nicholas Tomlinson (Clemson), Haonan Song (Lehigh)

**Project Duration:** 5/2024 – 5/2027

**Funding Source:** ARPA-e

#### Summary

This project aims to develop and test an ultrafast, noise-immune, versatile, efficient, reliable, scalable, and accurate light-controlled (UNIVERSAL) switch module. The proposed UNIVERSAL switch (US) module will be designed to provide fast protection meeting several key performance targets: 1) 20 kV/250 A ratings and LEGO-like scalability for higher voltage and current ratings. 2) 10X peak current capability and >99.9% efficiency using wide bandgap power semiconductors. 3) EMI noise-immune design with gate driving and sensing via optical means. 4) 500 V/ns and >200 A/ns ultrafast triggering slew rates. 5)  $\geq 30,000$  cycles lifetime operation and (N-2) fault-tolerant capability at full power using natural cooling and a redundant submodule design.

The project has three budget periods, each planned for 12 months. Tasks for the first budget period have been successfully completed. In Year 2 of the project, the primary focus will be on the design and testing of the US module's voltage and current sensors. The electrical and mechanical designs of the US module will be verified, and the designed components and key functional blocks will be experimentally integrated and validated within the SM, encompassing all electrical, thermal, mechanical, and optical aspects. The required SM-level di/dt and dv/dt performance targets will be achieved during this period. For the T2M activities, efforts will continue to refine the commercialization plan by mapping technical capabilities, identifying potential applications, and advancing the intellectual property strategy. The plan will be regularly updated to reflect progress, including engagement with prospective customers and reporting to ARPA-E on customer requirements and market insights.

The team is currently continuing low-power functional testing of the SM and US module-level sensors to validate the analysis. In parallel, work progressed on fabrication of the optical power supply, and preliminary test results have been obtained. Assembly of the SM, integrating components provided by different project partner organizations, is ongoing, and dynamic testing of the quarter-SM has been completed. Under the Technology-to-Market (T2M) activities, application scenario analysis was continued, demonstrating the feasibility of deploying the US module in next-generation power architectures, with specific emphasis on medium-voltage (e.g. 13.8 kV AC) data center distribution systems.

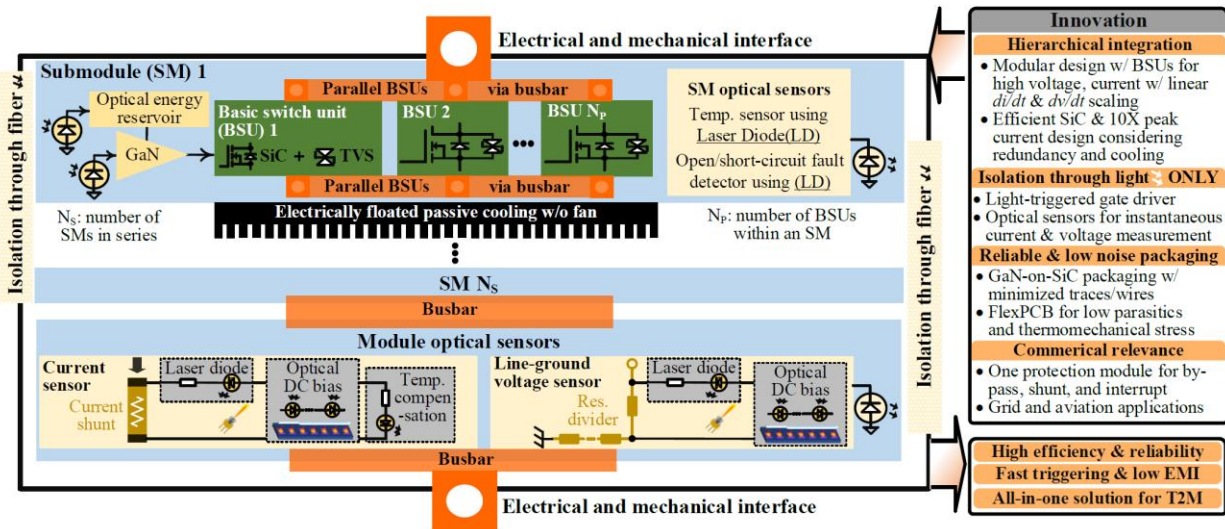


Fig. 1. Proposed US module with optical gating & sensing, passive air-cooling, & electrical/mechanical connection

### 37. SiC Based Modular Transformer-Less MW-Scale Power Conditioning System and Controller for Flexible Manufacturing Plants

**Project Lead:** Fred Wang (UTK), Yilu Liu (UTK), Leon Tolbert (UTK), Kevin Bai (UTK), Ruirui Chen (UTK)

**Graduate Students and Research associates:** Yang Xu (UTK), Jingxin Wang (UTK), Zihan Gao (UTK), Min Lin (UTK)

**Project Duration:** 10/2020 – 12/2025

**Funding Source:** DOE

#### Summary

The objective of this project is to develop a 10 kV SiC MOSFET-based 1 MW bi-directional power conditioning system (PCS) for manufacturing plants, consisting of back to back 13.8 kV AC/DC converters and a 200 kW isolated DC/DC converter connected to the PCS MV DC bus. The proposed PCS converter will meet performance targets including >99.4% power efficiency, <0.3 m<sup>3</sup>/MW volumetric density, >10% dispatchability, <\$30/kW cost (excluding SiC die cost), > 10 years lifetimes, 300 Hz voltage control bandwidth and >1 kHz current control bandwidth, and grid supporting functions.

Fig. 1-1 shows the PCS architecture. It serves as the interface between a 13.8 kV AC distribution grid and a manufacturing plant power system to enable various FMP architectures. With the PCS, an FMP power system can be operated as one or more AC asynchronous microgrid. With DC/DC converters ports interfacing directly with DC-fed loads and source, the FMP can also be operated as one or more hybrid AC asynchronous and DC microgrids. BP1 of this project has been completed in 2022, which focus on the design of this PCS and FMP controller. BP2 of this project has been completed in 2024, and the focus is to build and test one phase of the designed 1 MW back to back AC/DC/AC converter and one module of the designed 200 kW DC/DC converter.

During 2025-2026, all four 50 kW modules of the 10 kV SiC discrete device based 200 kW DC/DC converter are built and tested at rated voltage and power. All three phases of the 10 kV SiC module based 1 MW eight-level flying capacitor DC/AC converter are built. One phase-leg of the new Powex packaged 10 kV SiC module based five-level flying capacitor DC/AC converter is built and tested to 23 kV rated voltage. The materials for building another two phase-legs are prepared. The PCS integration strategy with MV testing platform and testing scenarios are determined.

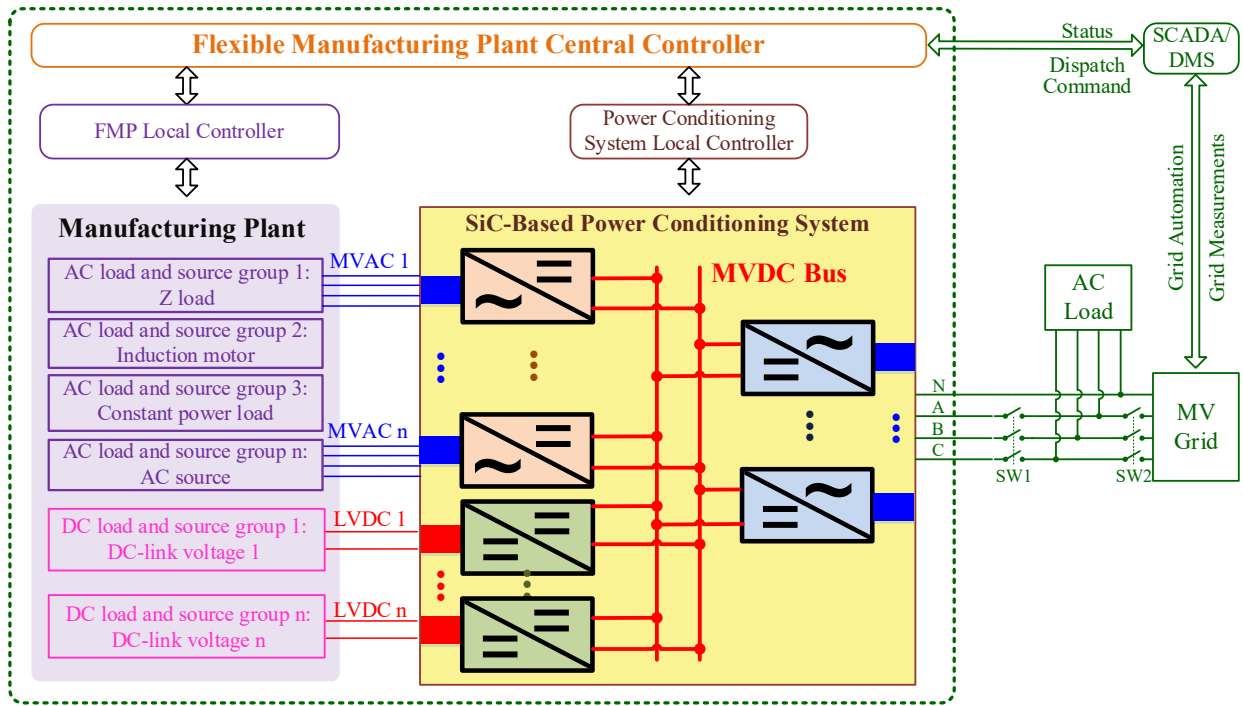


Fig. 1-1. PCS architecture for FMP system.

### 38. High Performance Isolated Dc/Dc Converter For Future Hvdc Data Center Application

<b>Project Lead:</b> Fred Wang (UTK)
<b>Graduate Students and Research faculty/associates:</b> Yanda Lyu (UTK)
<b>Project Duration:</b> 10/2025 – 9/2026
<b>Funding Source:</b> ABB

#### Summary

The project focuses on developing a high-efficiency, high-power-density isolated DC–DC converter for next-generation HVDC data center systems. The converter operates from a high-voltage DC input and delivers a nominal low-voltage output with large voltage ratio, targeting at high efficiency, high power density, and good transient performance.

Multiple converter topologies were evaluated, with emphasis on efficiency, scalability, and implementation complexity. Among the candidates, the LLC resonant converter was selected due to its inherent soft-switching capability, reduced component count, and suitability for high-frequency operation, all of which support high efficiency and compact design.

To meet system-level voltage and power demands, a modular input-series-output-parallel (ISOP) architecture based on LLC converters was adopted. This approach enables effective handling of high input voltage while maintaining manageable device stress and supporting scalable power integration.

A central challenge in this work is maintaining output voltage stability during fast load transients, given the unregulated nature of the LLC converter working as a DC transformer. The project therefore, investigates both control and design-level approaches to mitigate transient deviations while preserving efficiency.

The work will proceed toward prototype implementation and experimental validation, along with a systematic assessment of performance trade-offs to determine the suitability of the proposed architecture for future HVDC data center applications.